Human Molecular Genetics, 2014, Vol. 23, No. 11 **2858–2879**
doi:10.1093/hmg/ddt674
Advance Access published on January 9, 2014

c-Abl phosphorylates α-synuclein and regulates its degradation: implication for α-synuclein clearance and contribution to the pathogenesis of Parkinson's disease

Anne-Laure Mahul-Mellier[1], Bruno Fauvet[1], Amanda Gysbers[3], Igor Dikiy[4], Abid Oueslati[1], Sandrine Georgeon[2], Allan J. Lamontanara[2], Alejandro Bisquertt[5], David Eliezer[4], Eliezer Masliah[5], Glenda Halliday[3], Oliver Hantschel[2] and Hilal A. Lashuel[1,*]

[1]Laboratory of Molecular and Chemical Biology of Neurodegeneration, Brain Mind Institute, [2]ISREC Foundation Chair in Translational Oncology, Swiss Institute for Experimental Cancer Research, Ecole Polytechnique Fédérale de Lausanne, 1015 Lausanne, Switzerland, [3]Neuroscience Research Australia and the School of Medical Sciences, University of New South Wales, Randwick, Sydney, NSW 2031, Australia, [4]Department of Biochemistry and Program in Structural Biology, Weill Cornell Medical College, NY 10065, USA [5]Department of Neuroscience, University of California San Diego, La Jolla, CA, USA

Received October 17, 2013; Revised December 11, 2013; Accepted December 31, 2013

Increasing evidence suggests that the c-Abl protein tyrosine kinase could play a role in the pathogenesis of Parkinson's disease (PD) and other neurodegenerative disorders. c-Abl has been shown to regulate the degradation of two proteins implicated in the pathogenesis of PD, parkin and α-synuclein (α-syn). The inhibition of parkin's neuroprotective functions is regulated by c-Abl-mediated phosphorylation of parkin. However, the molecular mechanisms by which c-Abl activity regulates α-syn toxicity and clearance remain unknown. Herein, using NMR spectroscopy, mass spectrometry, *in vitro* enzymatic assays and cell-based studies, we established that α-syn is a *bona fide* substrate for c-Abl. *In vitro* studies demonstrate that c-Abl directly interacts with α-syn and catalyzes its phosphorylation mainly at tyrosine 39 (pY39) and to a lesser extent at tyrosine 125 (pY125). Analysis of human brain tissues showed that pY39 α-syn is detected in the brains of healthy individuals and those with PD. However, only c-Abl protein levels were found to be upregulated in PD brains. Interestingly, nilotinib, a specific inhibitor of c-Abl kinase activity, induces α-syn protein degradation *via* the autophagy and proteasome pathways, whereas the overexpression of α-syn in the rat midbrains enhances c-Abl expression. Together, these data suggest that changes in c-Abl expression, activation and/or c-Abl-mediated phosphorylation of Y39 play a role in regulating α-syn clearance and contribute to the pathogenesis of PD.

INTRODUCTION

The tyrosine kinase c-Abl is involved in regulating several cellular processes and has been implicated in the development of the central nervous system (1) by controling neurogenesis, neurite outgrowth and neuronal plasticity (2–7). More recently, increasing evidence from various experimental model systems has also revealed that c-Abl is activated in neurodegenerative diseases (8) such as Alzheimer's disease (AD) (9–11), Parkinson's disease (PD) (12,13), Niemann–Pick type C disease (14) and tauopathies (15). However, the mechanisms by which c-Abl contributes to the initiation and/or propagation of the pathogenic events underlying these neurodegenerative diseases remain poorly understood.

c-Abl is a 120 kDa protein belonging to the cytoplasmic tyrosine kinase family. Similar to Src kinases, c-Abl possesses

*To whom correspondence should be addressed at: Laboratory of Molecular and Chemical Biology of Neurodegeneration, Brain Mind Institute, Ecole Polytechnique Fédérale de Lausanne, 1015 Lausanne, Switzerland. Tel: +41 216939691; Fax: +41 216939665; Email: hilal.lashuel@epfl.ch

sequential SH3 and SH2 domains followed by a core catalytic domain with tyrosine kinase activity (16,17). Moreover, c-Abl has been detected in the nucleus and has a unique myristoylated N-terminal region that negatively regulates its kinase activity (16). The C-terminal region of c-Abl contains nuclear localization sequences and an F-actin-binding domain (16). c-Abl is a tightly regulated kinase and is activated through oxidative (18,19) or genotoxic stress (20), and the function of this protein is dependent on its subcellular localization (21–23). Cytoplasmic c-Abl regulates cellular adhesion and survival pathways, whereas c-Abl in the nucleus or in the mitochondria induces cell cycle arrest and apoptosis upon genotoxic stress (21,22,24).

Changes in c-Abl levels or activation have been linked to the pathogenesis of AD. For example, the level of activated c-Abl (c-Abl phosphorylated at Y412, which is a marker of high kinase activity) is higher than normal in the hippocampus of AD patients (25) and c-Abl colocalizes with AD pathology in both AD human brains and transgenic (tg) animal models (8,11). In addition, c-Abl activation has been directly associated with the molecular mechanisms that govern amyloid beta-induced toxicity in primary hippocampal cultures (25). Together, these studies indicate that c-Abl acts at different stages in the amyloid cascade and influences both amyloid toxicity and AD pathology, including the formation of granulovacuolar degeneration bodies and hyperphosphorylated tau (8,11,15).

Several lines of evidence have suggested that aberrant activation of c-Abl plays important roles in the pathogenesis of PD (12,13,26): (i) the c-Abl protein level is upregulated in postmortem striatum of PD patients (26) and the phosphorylation of c-Abl at Y412 is also enhanced in the substantia nigra (12,26) and striatum (12) of PD patients; (ii) two independent studies have shown that c-Abl phosphorylates parkin and impairs its E3 ligase activity, leading to loss of dopaminergic neurons in the substantia nigra (12,13); (iii) the inhibition of c-Abl activity by imatinib/Gleevec (27), nilotinib/Tasigna (28) or bafetinib/INNO-406 (29) protects against the loss of dopaminergic neurons in the substantia nigra of WT mice (12,26). More recently, Hebron *et al.* showed that c-Abl regulates the clearance of α-syn (26), a synaptic protein that has been strongly implicated in the pathogenesis of PD by evidence from genetic, pathological and animal modeling studies (30).

α-Syn is a 14 kDa protein that is found in the intraneuronal insoluble fibrillar aggregates called Lewy bodies (LBs) and Lewy neurites within the brains of patients diagnosed with PD (31,32) and other neurodegenerative α-synucleinopathies, including dementia with Lewy bodies (DLB) (33). The pathogenic relevance of α-syn aggregation and the mechanism by which these LBs are formed remain subjects of intense investigation and debate. However, the identification of missense mutations in the *SNCA* gene in some familial forms of PD and evidence that increased expression due to gene duplication or triplication is sufficient to cause familial forms of PD have reinforced the central role of this protein in the etiology of both sporadic and familial cases of PD (34–42). Recently, Hebron *et al.* provided evidence for a bidirectional relationship between α-syn and c-Abl *in vivo*, whereby an increase in α-syn expression induces the phosphorylation and subsequent activation of c-Abl, and conversely, an increase in the c-Abl expression and activity results in α-syn accumulation (26,43), suggesting that inhibition of c-Abl might constitute a viable strategy for attenuating α-syn accumulation and protecting against α-syn toxicity in PD. This hypothesis is supported by the observation that nilotinib increases α-syn clearance *via* the autophagy pathway and protects against α-syn-induced loss of dopaminergic neurons in a mouse model of PD (13,26). Nevertheless, the molecular mechanisms by which changes in c-Abl expression levels and/or activation regulate α-syn clearance and toxicity *in vivo* remain unknown.

Given our interest in the role of post-translational modifications in regulating α-syn functions in health and disease and previous observations demonstrating c-Abl-mediated neuroprotection in PD models, we sought to further explore the relationship between α-syn and c-Abl. Towards this goal, we sought to (i) determine whether α-syn is a physiological substrate of c-Abl, (ii) identify the tyrosine residues that are phosphorylated by c-Abl *in vitro* and validate our findings *in vivo* and (iii) determine the role of c-Abl-mediated phosphorylation in regulating α-syn clearance.

In this study, we demonstrate, for the first time, that α-syn is a *bona fide* substrate of c-Abl and showed that c-Abl phosphorylates α-syn, primarily at tyrosine 39 (Y39) and to a lesser extent at tyrosine 125 (Y125) *in vitro*, in neuroblastoma cell lines and in primary cultures of mouse cortical neurons. We also provide direct evidence that α-syn phosphorylated at Y39 is present in normal and PD human brain tissues. The phosphorylation of α-syn at Y39 can be abolished by using specific c-Abl inhibitors (imatinib, nilotinib and GNF-2) (44) or through the downregulation of c-Abl protein levels using siRNA. Conversely, the activation of c-Abl using DPH (5-[3-(4-fluorophenyl)-1-phenyl-1H-pyrazol-4-yl]-2,4-imidazolidinedione) (45) enhances α-syn phosphorylation at Y39. Moreover, the effects of c-Abl-mediated phosphorylation on α-syn clearance were also investigated.

RESULTS

c-Abl preferentially phosphorylates α-syn at Y39 in an *in vitro* kinase assay

α-syn contains four tyrosine residues (Y39, Y125, Y133 and Y136). Y125, Y133 and Y136 have previously been shown to undergo phosphorylation by several tyrosine kinases including c-Src (46), Fyn (47) and the Syk family (48). However, no kinase has been shown to phosphorylate α-syn at Y39. We first investigated whether c-Abl could be a tyrosine kinase for α-syn, using *in vitro* kinase assays. Purified α-syn was incubated in the presence or absence of a recombinant active c-Abl fragment comprising the SH2 and catalytic domains (residues 138–534), also known as SH2-CD c-Abl. In the presence of c-Abl, electrospray ionization mass spectrometry (ESI-MS) analysis showed the appearance of a new peak with a deconvoluted mass of 14 541 Da for WT α-syn, which is consistent with a single phosphorylation event (calculated mass: 14 540 Da) (Fig. 1A). Mutating Y39 to phenylalanine (Y39F) nearly abolished α-syn phosphorylation by c-Abl suggesting that Y39 is the primary and preferred site for c-Abl-mediated α-syn phosphorylation (Fig. 1A). In contrast, the Y125F mutant was efficiently phosphorylated at Y39 even to a higher extent than WT α-syn (Fig. 1A), suggesting that the phosphorylation at Y125 could decrease the propensity of c-Abl to phosphorylate α-syn at Y39. No phosphorylation was detected

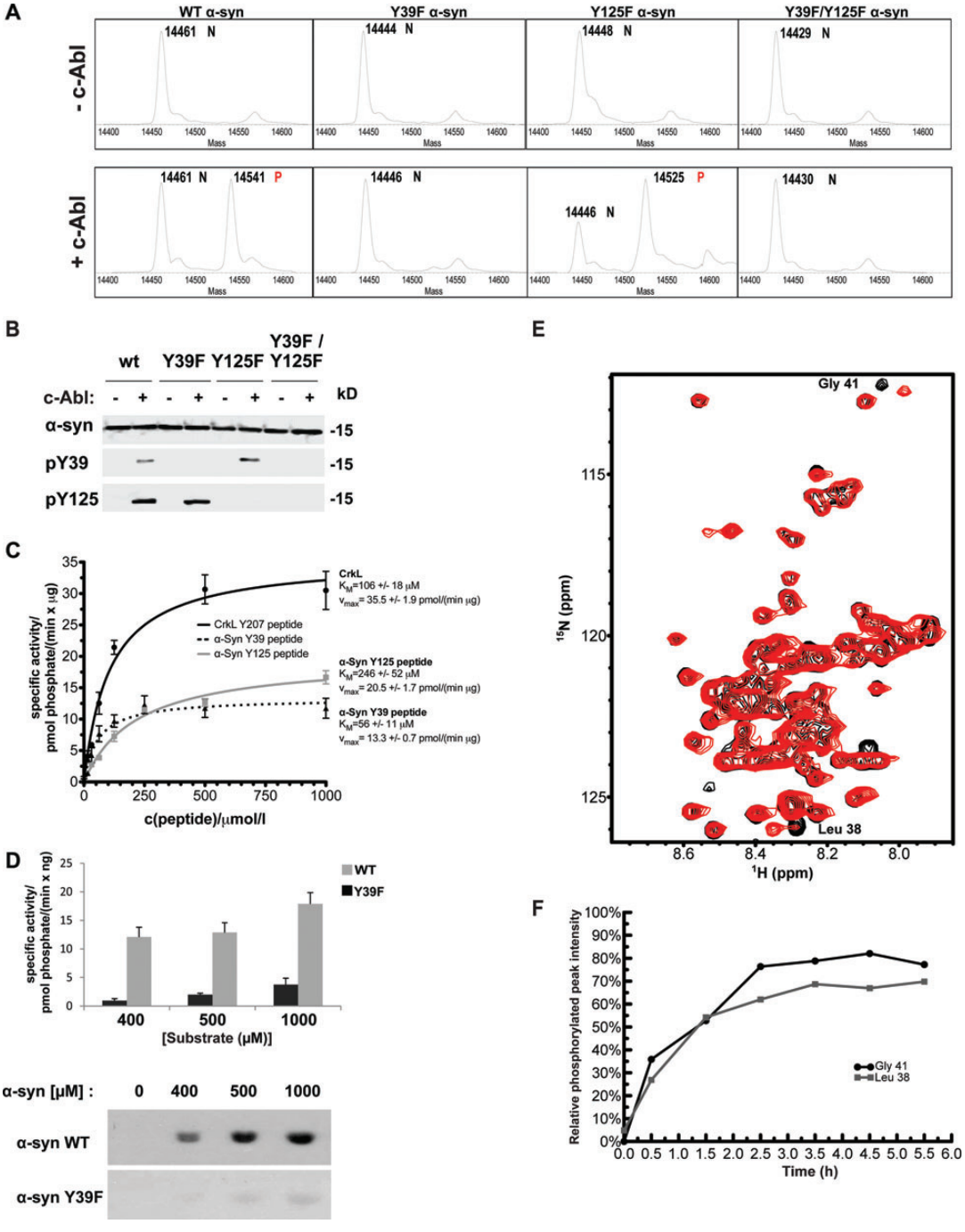

Figure 1. c-Abl preferentially phosphorylates α-syn at Y39 residue *in vitro*. (**A**) Mass spectrometry analysis of analytical *in vitro* phosphorylation assays of WT, Y39F, Y125F or the double mutant Y39F/Y125F α-syn with (+c-Abl) or without (−c-Abl) recombinant SH2-CD c-Abl. Phosphorylation was detected by a +80 Da mass shift. 'N' denotes nonphosphorylated starting material peaks, 'P' indicates the peaks corresponding to phosphorylated proteins. (**B**) WB analysis of the same reactions shown in (A) was performed using different phospho-specific α-syn antibodies in order to confirm that phosphorylation occurred at the expected sites. (**C**) Recombinant SH2-CD c-Abl kinase was used to perform kinase assays with increasing concentrations of α-syn peptides (dotted black line: biotin-α-syn (34–44)-NH_2; full gray line: biotin-α-syn (119–129)-NH_2) or the positive control CrkL peptide (full black line). Specific activity was calculated and plotted over the substrate concentration (Michaelis–Menten graph). The graph shows the mean ± SD of a representative experiment performed in triplicates. (**D**) Quantification of FL WT α-syn (dark gray bars) and Y39F (light gray bars) phosphorylation by recombinant WT SH2-CD c-Abl performed at different substrate concentrations (top panel). Bars represent the mean ± SD of a representative experiment performed in triplicates. Representative autoradiography (bottom panel) obtained from a SDS–PAGE gel from which the Coomassie-stained bands were cut and measured by scintillation counting to obtain the data in the top panel. (**E**) $^{1}H/^{15}N$ HSQC NMR spectrum of WT α-syn in the presence of c-Abl at $t = 0$ (black peaks) and after $t = 5–6$ h of phosphorylation (red peaks). The two-framed peaks in the upper right portion of the spectrum correspond to Gly41 in the unphosphorylated protein (black peak labeled '#') and in the Y39-phosphorylated form (red peak labeled '*'). (**F**) Kinetics of α-syn phosphorylation at Y39 measured by NMR. The phosphorylation-dependent chemical shift changes of Gly41 (see panel C) and Leu 39 (see Supplementary Material, Fig. S1B) were used to quantify phosphorylation at Y39 as the intensity of the peak arising from the phosphorylated protein relative to the sum of the intensities of the peaks arising from both phosphorylated and unphosphorylated protein. Values <0 (due to noise-related negative peak intensities) were set to 0.

for the Y39F/Y125F double mutant (Fig. 1A, bottom panel), suggesting that c-Abl does not significantly phosphorylate α-syn at Y133 or Y136. These results show that Y39 is the primary residue phosphorylated by c-Abl *in vitro*.

To characterize α-syn phosphorylation at Y39 in cells and brain tissues, we generated an anti-pY39 α-syn antibody against a synthetic peptide (amino acids 34–45) harboring the phosphate group at Y39. No previous reports described the availability or use of anti-pY39 antibodies. The specificity of this antibody for pY39 α-syn was validated using a peptide-based dot blot assay (Supplementary Material, Fig. S1A and B) and confirmed by western blot (WB) analysis of mammalian cell lines (Supplementary Material, Fig. S1C). We further investigated the specificity of the pY39 antibody using immunohistochemistry (IHC) (Supplementary Material, Fig. S1E and F) or immunocytochemistry (ICC) (Supplementary Material, Fig. S1G) in hippocampal primary neurons. For IHC, we used brains from PDGF-α-syn tg mice (49), displaying abundant α-syn accumulation in the neocortex and limbic system (α-syn tg), or α-syn KO mice (α-syn KO). As shown in Fig. S1E, the pY39 signal was detectable only in tg mice overexpressing α-syn and was totally absent in brains in which α-syn is not expressed (KO mice). Similar results were obtained in primary hippocampal neurons from WT or α-syn KO mice (Supplementary Material, Fig. S1G). Moreover, when the pY39 antibody was preincubated with a specific blocking peptide, no positive signal was detected by WB (Supplementary Material, Fig. S1D) or by IHC (Supplementary Material, Fig. S1F) in tg mouse tissues. Taken together, these results establish the specificity of the anti-pY39 antibody used in this study.

WB analysis of samples of recombinant α-syn *in vitro* phosphorylated by active SH2-CD c-Abl confirmed α-syn phosphorylation at Y39 and Y125 residues (Fig. 1B), consistent with the results obtained by mass spectrometry (MS) (Fig. 1A). Nevertheless, neither intact-protein MS nor WBs using phospho-specific antibodies allowed quantitative comparison of the relative affinities of c-Abl toward each site. Therefore, we performed *in vitro* quantitative radiometric assays of α-syn phosphorylation by measuring ^{32}P incorporation from γ-^{32}P ATP and compared the K_M of c-Abl toward Y39 and Y125 using recombinant WT SH2-CD c-Abl. We first used peptides as substrates: α-syn (34–44) and α-syn (119–129), spanning the Y39 and Y125 sites, respectively, as well as a peptide from the canonical c-Abl substrate CrkL that was used as a positive control and a point of reference. As shown in Figure 1C, c-Abl displayed a higher affinity for the Y39 peptide (α-syn (34–44)) ($K_M = 56 \pm 11$ μM) than for the Y125 peptide (α-syn(119–129)) ($K_M = 246 \pm 52$ μM), thus suggesting a marked preference for phosphorylation at Y39 than at Y125 (Fig. 1C). The measured K_M and V_{max} values for the α-syn peptides (Fig. 1C) were in a similar range to the CrkL peptide, indicating that α-syn can be considered as a good c-Abl substrate.

In order to take into account the possibility that the binding of c-Abl to α-syn could involve amino acid residues that are distant from the phosphorylation sites, we also performed *in vitro* kinase assays using recombinant full-length (FL) α-syn as substrate and FL human CrkII as a reference. These experiments confirmed that Y39 is the main c-Abl phosphorylation site in FL α-syn because the Y39F mutant showed limited signals (Fig. 1D). These findings demonstrated that c-Abl is a reasonably efficient kinase that phosphorylates α-syn: although the well-known c-Abl substrate CrkII (50) was more efficiently phosphorylated by SH2-CD c-Abl than α-syn (Supplementary Material, Fig. S2A). However the range in protein concentration to obtain signal was comparable between the two proteins (Supplementary Material, Fig. S1A). It is worth mentioning that the high protein concentrations required to obtain good signals compared with the peptide-based experiments (Fig. 1C) could possibly be explained by a decreased accessibility of the phosphorylation sites owing to stabilization of the intramolecular C- and N-terminal interactions of monomeric α-syn (51) or formation of α-syn oligomers.

c-Abl-mediated α-syn phosphorylation at Y39 was also confirmed using real-time nuclear magnetic resonance (NMR) spectroscopy performed at pH 6.8 (Fig. 1E) and pH 7.4 (Supplementary Material, Fig. S2B). ^{15}N-labeled WT α-syn was co-incubated with recombinant c-Abl, and phosphorylation at Y39 was measured in real time through the sequential acquisition of short (1 h) ^{1}H–^{15}N HSQC spectra (Fig. 1E and Supplementary Material, Fig. S2B), where the appearance of new cross-peaks for residues L38 and G41 (among others) reports on the phosphorylation at Y39. Maximum phosphorylation was achieved within 3–4 h with a final conversion estimated at 70–80% (Fig. 1F). No clear spectral changes were observed for residues near Y125, suggesting little or no phosphorylation at this site, but the relevant region of the spectrum was highly crowded, so a definitive conclusion is not possible based solely on the present NMR data. Together, these data provide strong evidence that α-syn is a good substrate for c-Abl and that Y39 is the major phosphorylation site, while the extent of Y125 phosphorylation remained low under these *in vitro* conditions.

Both Y39 and Y125 residues are phosphorylated in human PD brains and in α-syn tg mice

Next, we sought to determine whether phosphorylation of α-syn at Y39 occurs *in vivo,* and we further explored the relationship between c-Abl and α-syn in healthy and PD human brains. The anterior cingulate cortex was chosen for analysis, as this region has been shown to have increased α-syn phosphorylation at the first indication of Lewy Body pathologies in the olfactory bulb and substantia nigra (52), with the degree of phosphorylation correlating with the severity of Lewy body formation (53). This region has limited cell loss in PD and can therefore be structurally compared with control tissue. In addition to detecting phosphorylated forms of α-syn (including pY39, pY125 and pS129 as a positive marker for PD caes), we also assessed and compared the levels of c-Abl in PD brains and age-matched control cases (Fig. 2 and Table 1).

The phosphorylation levels (pS129, pY125 and pY39) of α-syn were evaluated using WB (Fig. 2A, left panel; shown, $n = 7$ from PD cases and $n = 7$ from age- and post-mortem delay-matched neurological and neuropathological controls) and quantified by densitometry ($n = 17$ from PD cases and $n = 17$ from control samples) (Fig. 2A, right panel). pY125 and pY39 were detected at similar levels in the anterior cingulate cortex from PD ($n = 17$) and age- and post-mortem delay-matched neurological and neuropathological controls ($n = 17$), whereas, as expected, pS129 was detected only in PD cases (Fig. 2A). α-syn phosphorylated at Y39 and/or Y125 was detected only in the sodium dodecyl sulfate (SDS) soluble fraction of the anterior cingulate cortex and putamen from PD cases (Fig. 2B).

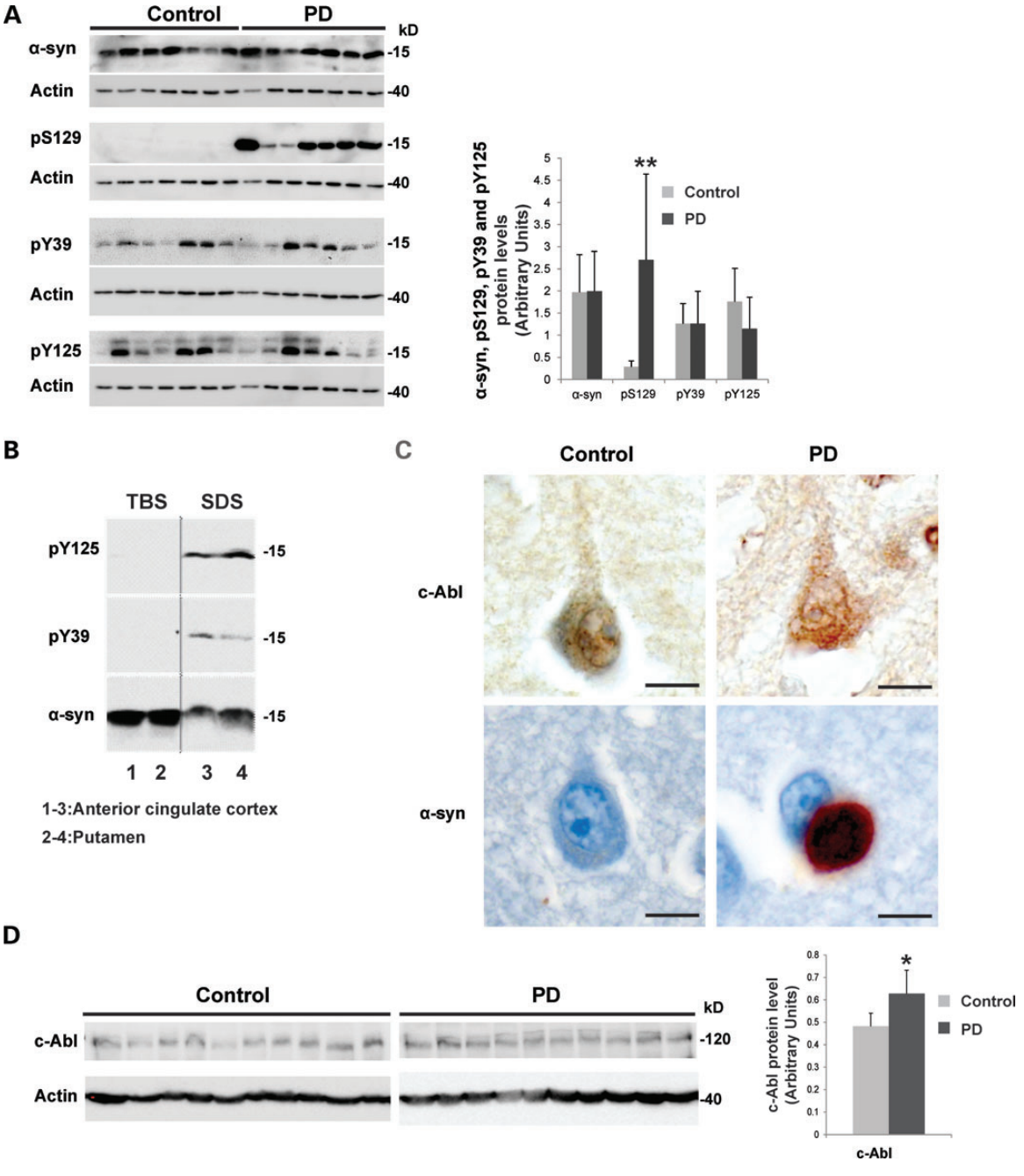

Figure 2. Phosphorylation of α-syn at Y39 and Y125 and an increase in c-Abl protein level can be detected *in vivo* in human PD brain tissue. (**A**) Representative WB of the relative phosphorylation status of α-syn observed in PD cases versus controls. Protein extracts from samples of the anterior cingulate cortex from Parkinson's disease patients ($n = 17$) and age- and post-mortem delay-matched neurological and neuropathological controls ($n = 17$) were resolved by SDS–PAGE and analyzed by WB (shown, $n = 7$ from PD cases and $n = 7$ from age- and post-mortem delay-matched neurological and neuropathological controls) using α-syn antibodies against pS129, pY125, pY39 and total α-syn (left-hand-side panel). Phosphorylation levels (pS129, pY125, pY39) of α-syn were evaluated by densitometry quantification (right-hand-side panel). The band intensities were normalized in the following manner: [(pY39 or pY125 or pS129/actin)/α-syn]. The bars represent the mean ± SD of PD cases ($n = 17$) and control cases ($n = 17$). $^{**}P < 0.005$; (Student's *t*-test: PD cases versus controls). (**B**) Representative WB of the relative amounts of α-syn in PD cases. The brain tissue (anterior cingulate cortex that has lots of Lewy bodies (lanes 1 and 3) and putamen where the dopamine terminals are lost (lanes 2 and 4) from PD cases was sequentially extracted for TBS-soluble and SDS-soluble fractions. Proteins were resolved by SDS–PAGE and analyzed by WB using α-syn antibodies against pY125, pY39 and total α-syn. (**C**) Representative fixed tissue ICC showing protein immunoreactivity in PD and control cases. c-Abl immunoreactivity was observed in small neuronal cytoplasmic punctate structures, which were enhanced in a proportion of pyramidal neurons in PD cases versus controls. α-syn immunoreactive Lewy bodies were only observed in a proportion of pyramidal neurons in the PD cases. Scale bar = 10 μm. (**D**) Representative WB of the relative c-Abl protein amounts observed in PD cases versus controls. Protein extracts from samples of the anterior cingulate cortex from PD cases ($n = 17$) and age- and post-mortem delay-matched neurological and neuropathological controls ($n = 17$) were resolved by SDS–PAGE and analyzed by WB (shown, $n = 10$ from PD cases and $n = 10$ from age- and post-mortem delay-matched neurological and neuropathological controls) using a c-Abl antibody (left hand panel). c-Abl protein level was evaluated by densitometry quantification (right-hand-side panel). The band intensities were normalized in the following manner: (c-Abl/actin). The bars represent the mean ± SD of PD cases ($n = 17$) and control cases ($n = 17$). $^{*}P < 0.05$; (Student's *t*-test: PD cases versus controls).

Table 1. Demographic details for PD and control cohorts

Diagnosis	Sex (M:F)	Age (years)	PMD (h)	Duration (years)
PD ($n = 17$)	13:4	78.9 ± 1.2 (69–88)[a]	18.3 ± 3.2 (5–50)[a]	15.3 ± 1.7 (7–33)
Control ($n = 17$)	8:9	78.1 ± 2.7 (60–97)	17.8 ± 2.6 (5–36)	

Values are given as mean ± standard error and range for age at death (age), post-mortem delay (PMD) and disease duration (duration).
[a]Not significantly different from control values (*t*-test, $P > 0.05$).

Interestingly, IHC revealed c-Abl expression in small neuronal cytoplasmic punctate structures, which were enhanced in a proportion of pyramidal neurons in PD cases versus controls (Fig. 2C, upper panel). To the best of our knowledge, this is the first report showing the presence of c-Abl within α-syn aggregates in human brain tissue from PD patients. WB (shown, $n = 10$ from PD cases and $n = 10$ from age- and post-mortem delay-matched neurological and neuropathological controls) and densitometry quantification showed a slight, but significant, increase in c-Abl protein levels in the anterior cingulate cortex from PD patients ($n = 17$) compared with age- and post-mortem delay-matched neurological and neuropathological controls ($n = 17$) (Fig. 2D). These data are consistent with the recent findings of Hebron *et al.*, which showed an increase in c-Abl protein levels in the striatum of brains from post-mortem PD patients (26).

The levels of c-Abl, pY39 and pY125 α-syn proteins were also assessed in tg mice overexpressing human WT α-syn under the mThy1 promoter (mThy1-α-syn, Line 61) (54). These mice develop behavioral motor deficits (40), axonal pathology and accumulation of α-syn cleaved at the C-terminus, and aggregate within cortical and subcortical regions (55) mimicking the pathological aggregates of PD/DLB (56,57). WB analysis of membrane fractions of brain homogenates from non-tg and α-syn WT tg mice revealed a significant increase in protein levels of c-Abl, pY39 and pY125 α-syn as well as total α-syn levels (Fig. 3A). However, cytosolic fractions did not show positive signals (Supplementary Material, Fig. S3A). Antibodies against pY39 and pY125 α-syn displayed increased immunoreactivity in neurons in the deeper layers of the temporal cortex (Fig. 3B, left hand panel). In some cases, the immunostaining concentrated in the cytoplasm was mimicking inclusions (Fig. 3B, left hand panel). Interestingly, c-Abl immunostaining in pyramidal neurons in the neocortex was increased in the α-syn tg mice compared with the WT mice (Fig. 3B, right hand panel). Together, these data show that c-Abl levels are increased in diseased human brains and in a mice model of PD.

c-Abl protein levels are transiently increased in a rat genetic model of PD

The protein levels of c-Abl, pY39 and pY125 were then investigated in rat midbrain in which α-syn has been overexpressed using the AAV-delivery system in the substantia nigra (58,59) (Fig. 4). Strikingly, 1 month after injection, c-Abl protein levels were significantly increased in the soma and the neurites of dopaminergic neurons within the substantia nigra overexpressing α-syn ($n = 3$, Fig. 4A and B). Similar observations were made using three different antibodies raised against different epitopes in c-Abl (Fig. 4A and B). Interestingly, c-Abl signal was significantly reduced 3 months after injection ($n = 3$, Fig. 4A and B), suggesting that c-Abl expression is transiently induced by the overexpression of α-syn. No positive signal was detected in the non-injected side or in the control group (FPmax-injected rats; Fig. 4A and B), suggesting that under physiological conditions, c-Abl is expressed at low levels and/or its levels are tightly regulated (8,26). The use of specific antibody against activated c-Abl (pY412) revealed that upon α-syn overexpression the level of activated c-Abl was increased (Fig. 4C, top panel). Moreover, an increase in pY39 α-syn levels was also observed (Fig. 4C, bottom panel).

Taken together, these data demonstrate that α-syn overexpression induces a transient increase of c-Abl expression that is associated with the accumulation of activated c-Abl and phosphorylated α-syn at Y39.

c-Abl induces α-syn phosphorylation at Y39 and Y125 in primary cortical neurons

Next, we investigated whether c-Abl could phosphorylate endogenous α-syn at Y39 in primary cortical neurons. Figure 5A demonstrates that endogenous mouse α-syn was phosphorylated at Y39 and Y125. This basal phosphorylation level at both residues was significantly increased in cortical neurons after transduction with lentiviruses encoding WT c-Abl (Fig. 5A). Phosphorylation of α-syn by c-Abl was then examined using ICC (Fig. 5B). Primary cortical neurons (WT and α-syn KO) were transduced with lentiviruses to express WT c-Abl or KD c-Abl (an inactive form of c-Abl bearing the K290R point mutation in the kinase domain). At 5 days post-infection, c-Abl efficiently phosphorylated α-syn at Y39 and Y125 residues in WT mouse cortical neurons (Fig. 5B). Moreover, the kinase-dead form of c-Abl (KD c-Abl) was not able to phosphorylate WT α-syn (Supplementary Material, Fig. S3). As expected, cortical neurons of α-syn KO mice showed no immunoreactivity with the antibodies specific for either pY39 or pY125 α-syn (Fig. 5B and Supplementary Material, Fig. S3B), further confirming the specificity of the antibodies used in this study.

c-Abl induces α-syn phosphorylation at Y39 and Y125 in mammalian cells

For detailed biochemical analyses of the interplay between α-syn and c-Abl, we used HEK293T, HeLa and the neuroblastoma cell line M17. We first characterized c-Abl-mediated α-syn phosphorylation in these cell lines. As endogenous α-syn expression is hardly detectable by WB in these cell lines, HEK293T cells were co-transfected with WT α-syn or mutants in which one or multiple tyrosine residues were mutated from tyrosine to phenylalanine (Y39F, Y125F and Y39F/Y125F) together

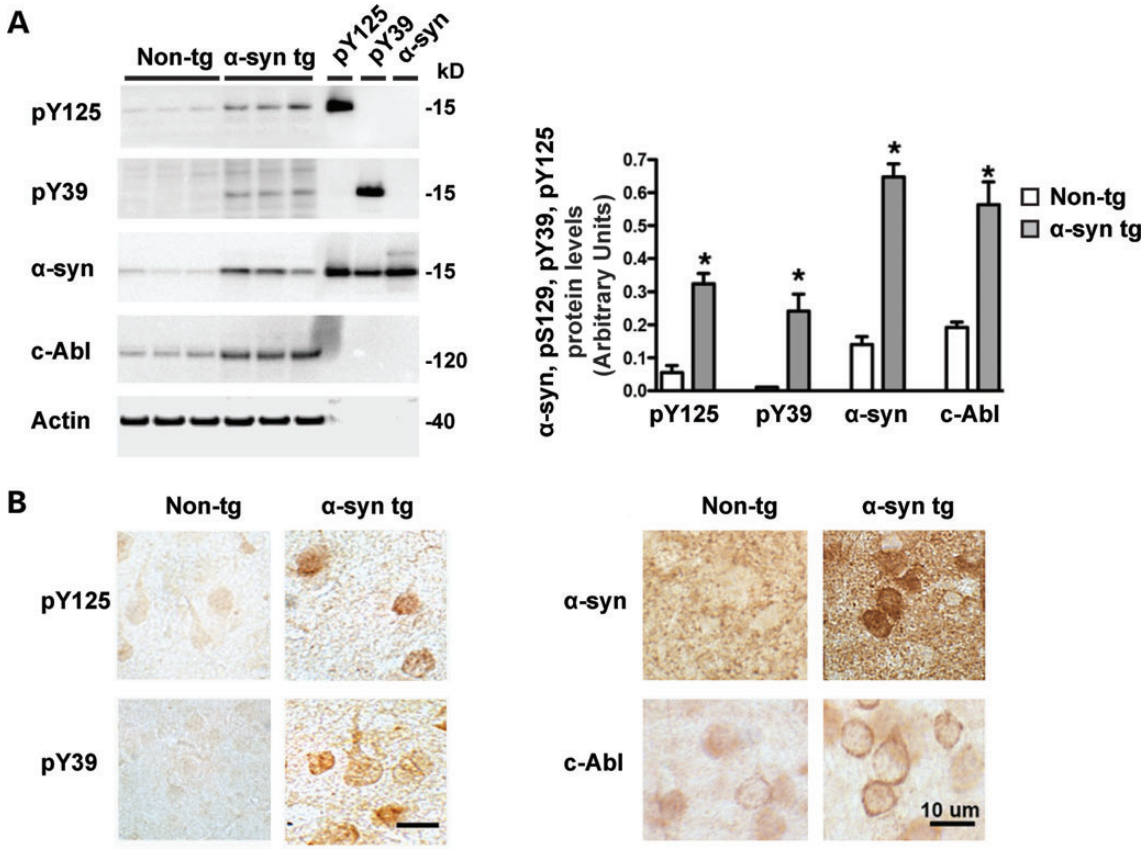

Figure 3. Both c-Abl and phosphorylated α-syn (at Y39 or Y125) levels are increased in α-syn transgenic mice. (**A**) Brain homogenates from non-transgenic and mThy1-h α-syn WT transgenic (tg) mice from line 61 (49) (male, 6 m/o) were fractioned into membrane and cytosolic fractions and ran in SDS–PAGE gels, blotted and probed with antibodies against pY125, pY39, α-syn, c-Abl and actin as previously described (54). Representative blots are from the membrane fraction, bands in the far right are recombinant proteins that served as positive controls and molecular weight markers (left-hand-side hand panels). Image analysis of the specific bands expressed as ratio to the actin loading control. The bars represent the mean ± SD of $n = 5$ mice per group, $^{*}P < 0.001$ by Student's *t*-test. (**B**) Immunocytochemical analysis with antibodies pY125, pY39, α-syn and c-Abl developed with diaminobenzidine utilizing vibratome sections. Images are representative of the temporal cortex. In the tg mice, there was increased immunoreactivity in neuronal cell bodies with pY125, pY39, α-syn and c-Abl antibodies.

with c-Abl or a control plasmid encoding luciferase (LUC). WB (Fig. 6A and B) and ICC (Fig. 6C) analyses showed the phosphorylation of both Y39 and Y125 residues by c-Abl in HEK293T cells. When WT or Y39F α-syn was expressed, we observed only tyrosine phosphorylation at Y125. However, when WT α-syn was coexpressed with c-Abl, a prominent band was also detected using the anti-pY39 antibody. As observed in cortical neurons, the kinase inactive form of c-Abl (KD c-Abl) did not phosphorylate WT α-syn, whereas the constitutively active form of c-Abl (bearing the P242E/P249E double mutation; referred to as PP c-Abl) phosphorylates α-syn more efficiently (almost a 2.5-fold increase) at Y39 and Y125 compared with WT c-Abl (Fig. 6B). The ability of c-Abl to phosphorylate α-syn at Y39 and Y125 was also confirmed in HeLa (Supplementary Material, Fig. S4A and C) and M17 cell lines (Supplementary Material, Fig. S4B).

Modulation of c-Abl level or activity directly influences the level of α-syn phosphorylation at Y39 and Y125

Our cell-based experiments confirmed that α-syn is a potential physiologically relevant substrate for c-Abl. To confirm the specificity of c-Abl-mediated α-syn phosphorylation at Y39 and Y125, we modulated c-Abl activity in cells through the downregulation of c-Abl protein expression using siRNA or by pharmacological inactivation or activation of c-Abl kinase activity.

We first validated the efficiency and specificity of the siRNAs designed to downregulate c-Abl in HEK293T cells. As shown in Figure 7A, 48 h after transfection, c-Abl siRNAs reduce the endogenous c-Abl protein levels by ∼60%. The use of a Scramble (Sc) siRNA sequence did not affect c-Abl protein levels, confirming the specificity of the designed c-Abl siRNA (Fig. 7A).

We then sought to investigate whether α-syn phosphorylation induced by c-Abl overexpression could be attenuated by c-Abl siRNA downregulation. As expected, when the level of c-Abl overexpressed in HEK293T cells was downregulated to approximately endogenous c-Abl levels (Fig. 7A), the phosphorylation of α-syn at Y39 and Y125 was nearly abolished (Fig. 7B).

We then assessed the effect of inhibiting c-Abl activity using three highly specific c-Abl inhibitors: nilotinib, imatinib (ATP-competitive kinase inhibitors) (60) and GNF-2 (allosteric c-Abl inhibitor) (61). All three inhibiors strongly decreased α-syn phosphorylation levels at Y39 and at Y125 (Fig. 7C). On the contrary, activation of endogenous c-Abl using the allosteric activator DPH (45) resulted in a marked increase in α-syn phosphorylation at Y39 and Y125 in SH-SY5Y cells (Fig. 7D).

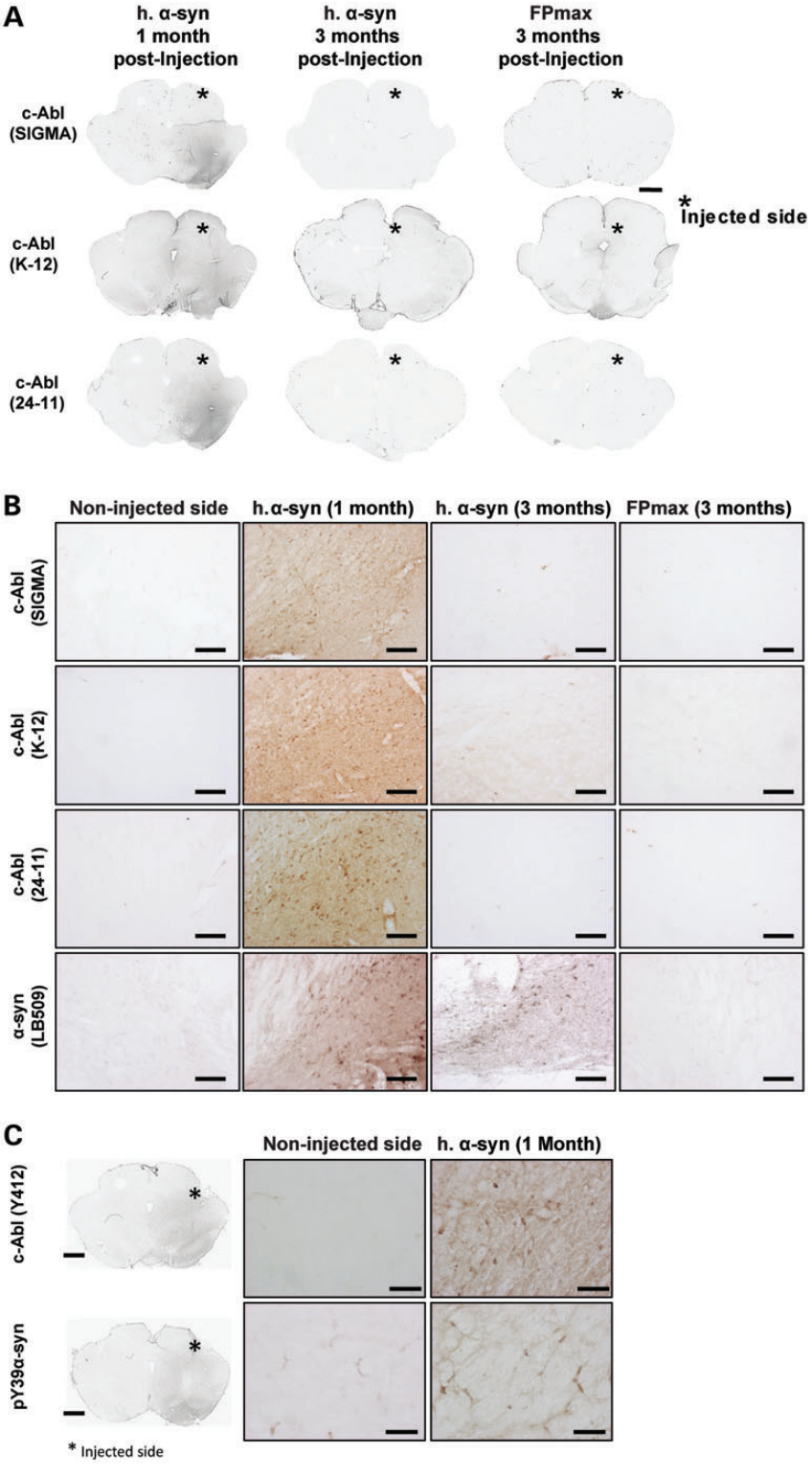

Figure 4. c-Abl protein levels increase transiently upon α-syn overexpression in rat midbrains. (**A** and **B**) Effect of α-syn overexpression on c-Abl protein levels *in vivo*, low magnification (scale bar: 500 μm) (A) and high-power magnification photomicrographs (scale bar: 100 μm) (B) that illustrate the endogenous protein level of c-Abl after the overexpression of human α-syn or FPmax (*, injected side; $n = 3$ per condition). The use of three different antibodies raised against different epitopes of c-Abl [(Sigma), (K12, Santa Cruz), (24-11, Santa Cruz)] revealed a dramatic increase of c-Abl protein level only in the side injected with human α-syn. Overexpression of α-syn was confirmed by IHC staining on serial section (B, bottom line). No c-Abl signal was detected in FPmax-injected or in the non-injected sides. The enhancement of c-Abl protein expression induced by α-syn overexpression was primarily observed at 1 month post-injection and disappeared after 3 months post-injection, suggesting a transient interplay between c-Abl and α-syn. (**C**) Protein levels of pY39 α-syn and activated c-Abl (pY412, a marker of high kinase activity) increased only in the injected side overexpressing α-syn 1 month post-injection (scale bar: 50 μm).

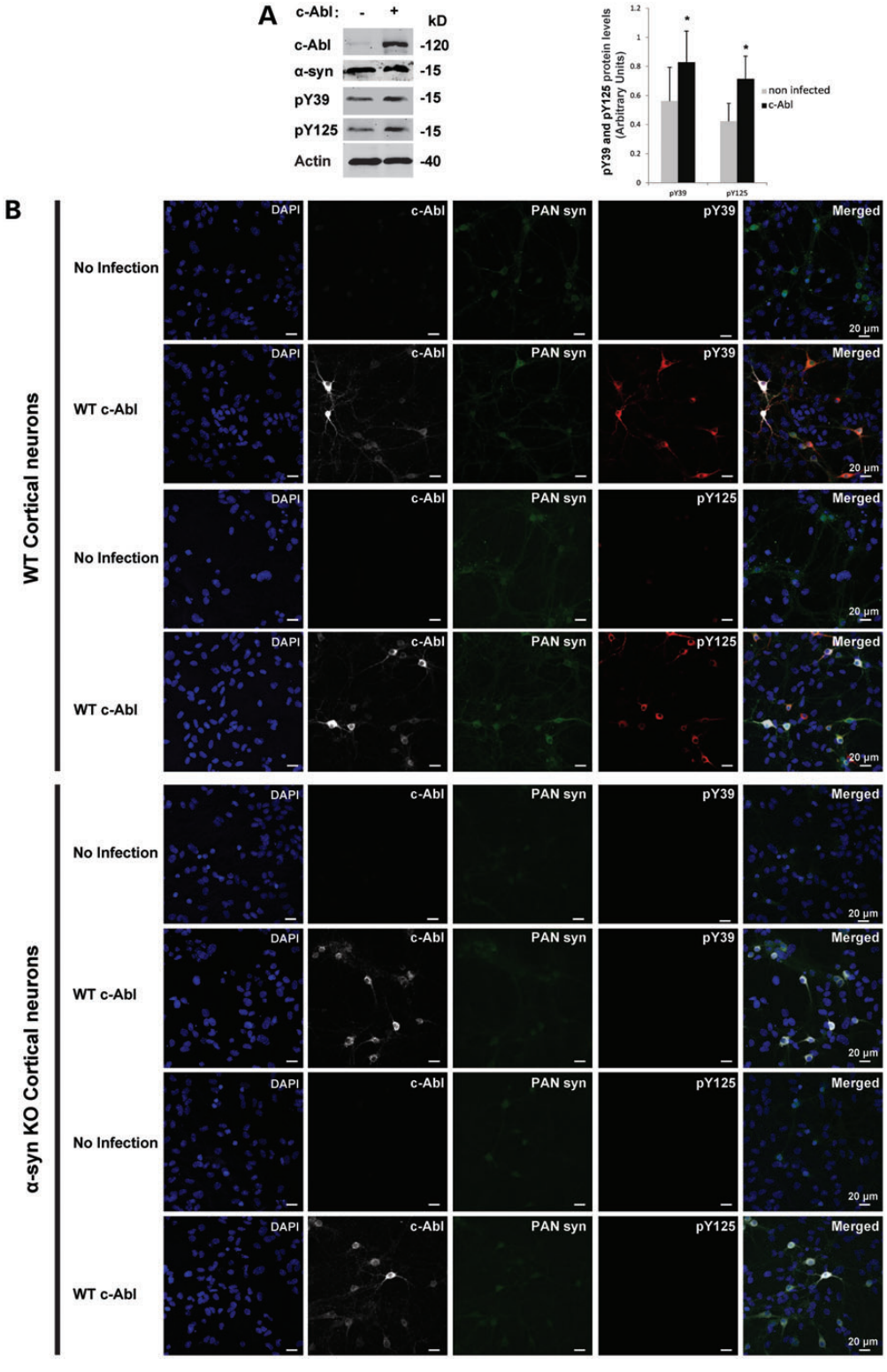

Figure 5. c-Abl induces α-syn phosphorylation at Y39 and Y125 residues in primary cortical neurons. (**A**) WT primary cortical neurons were infected with lentivirus encoding for c-Abl or with an empty lentivirus. Five days post-infection, neurons were lysed and the proteins were separated using SDS–PAGE and detected by WB analysis (left-hand-side panel). The α-syn phosphorylation status was assessed using the phosphorylation site-specific antibodies for Y39 or Y125 residues. α-syn and c-Abl expressions were confirmed in an additional protein blot using specific antibodies. Actin was used as a loading control. The phosphorylation of α-syn at residues Y39 and Y125 was evaluated by densitometry quantification (right-hand-side panel). The band intensities were normalized in the following manner: pY39/[α-syn/actin] or pY125/[α-syn/actin]. Bars represent the mean ± SD of three independent experiments. $^{*}P < 0.05$ (Student's *t*-test: non-infected versus c-Abl infection). (**B**) WT or α-syn KO primary cortical neurons were infected with c-Abl lentivirus or an empty lentivirus. Five days post-infection, neurons were immunostained with the appropriate antibodies and counterstained with DAPI to reveal the nucleus.

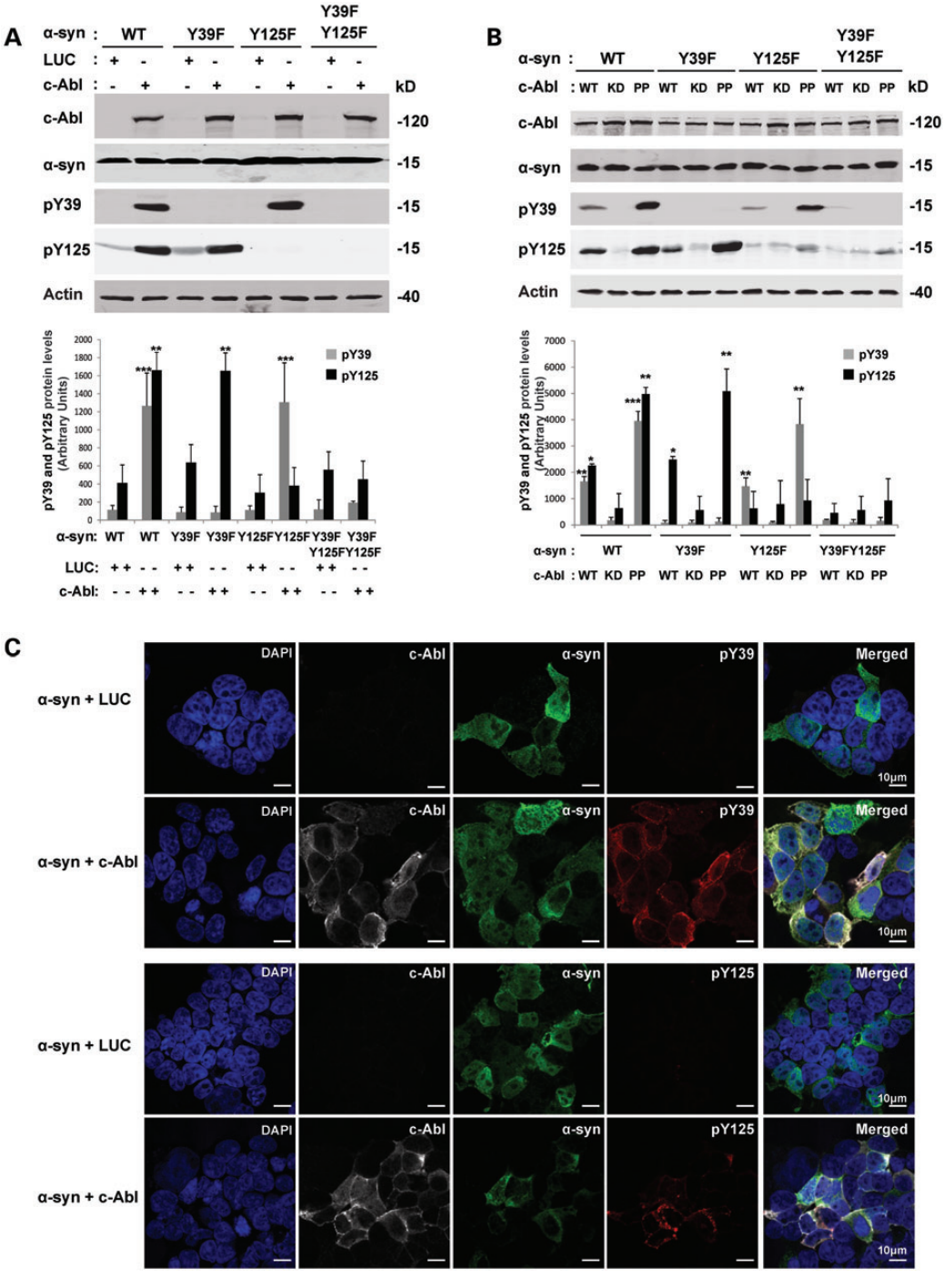

Figure 6. c-Abl induces α-syn phosphorylation at Y39 and Y125 residues in HEK293T cells. (**A**) HEK293T cells were transfected with WT α-syn or its mutants (Y39F, Y125F or Y39FY125F) together with plasmids encoding for LUC (negative control) or WT c-Abl. Twenty-four hours post-transfection, cells were lysed and the proteins separated using SDS–PAGE and detected by WB analysis (top panel). α-syn phosphorylation status was assessed using phosphorylation site-specific antibodies for Y39 or Y125 residues. α-syn and c-Abl expression were confirmed in an additional protein blot using specific antibodies. Actin was used as a loading control. The phosphorylation of α-syn at residues Y39 and Y125 was evaluated by densitometry quantification (bottom panel). The band intensities were in the following manner: pY39/[α-syn/actin] or pY125/[α-syn/actin]. The bars represent the mean ± SD of three independent experiments. $^{**}P < 0.005$; $^{***}P < 0.0005$ (Student's *t*-test: α-syn + LUC versus α-syn + c-Abl). (**B**) HEK293T cells were transfected with WT α-syn or its mutants (Y39F, Y125F or Y39FY125F) together with plasmids encoding for WT c-Abl or its inactive mutant KD c-Abl (kinase dead) or its constitutively active mutant PP c-Abl. Twenty-four hours post-transfection, cells were lysed and proteins separated using SDS–PAGE and detected by WB analysis (top panel). α-syn phosphorylation status was assessed using phosphorylation site-specific antibody for Y39 or Y125 residues. α-syn and c-Abl expression were confirmed in an additional protein blot using specific antibodies. Actin was used as a loading control. Phosphorylation of α-syn at residues Y39 and Y125 was evaluated by densitometry quantification (bottom panel). The band intensities were normalized as followed: pY39/[α-syn/actin] or pY125/[α-syn/actin]. The bars represent the mean ± SD of three independent experiments. $^{**}P < 0.005$; $^{***}P < 0.0005$ (Student's *t*-test: α-syn + KD c-Abl versus α-syn + WT c-Abl or PP). (**C**) HEK293T cells were transfected with WT α-syn together with plasmids encoding for LUC or WT c-Abl. Twenty-four hours post-transfection, cells were immunostained with the appropriate antibodies and counterstained with DAPI to reveal the nucleus.

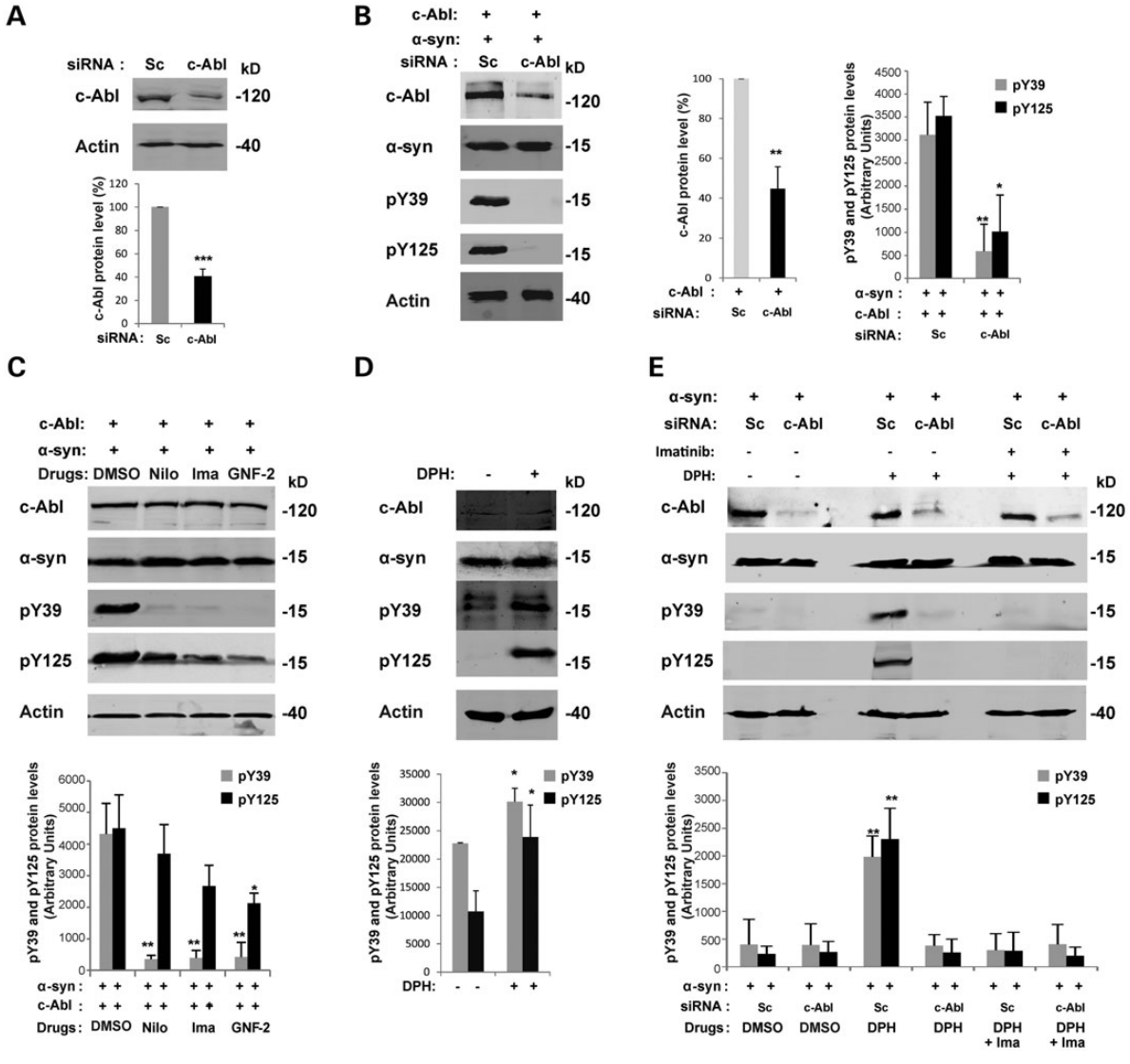

Figure 7. Modulation of c-Abl activity regulates α-syn phosphorylation at Y39 and Y125 residues. (**A**) Validation of the siRNA against c-Abl. HEK293T cells were transfected with specific siRNA against c-Abl or with a negative control (scramble siRNA, Sc). Forty-eight hours post-transfection, cells were lysed and protein level of endogenous c-Abl was assessed by WB and quantified by densitometry. The band intensities were normalized in the following manner: c-Abl/actin. The bars represent the mean ± SD of four independent experiments. $^{***}P < 0.005$ (Student's *t*-test: siRNA Sc cells versus siRNA c-Abl cells). (**B**) Downregulation of c-Abl protects α-syn from phosphorylation at Y39 and Y125 residues. HEK293T cells were transfected with a siRNA construct against c-Abl or with a control scrambled siRNA (Sc) together with plasmids encoding for WT α-syn and WT c-Abl. The downregulation of the c-Abl protein and its effect on α-syn phosphorylation (Y39 and Y125 residues) was confirmed by WB 48 h post-transfection (left-hand-side panel). Actin was used as a loading control. α-syn phosphorylation at Y39 and Y125 was evaluated by densitometry quantification (right-hand-side panel). The band intensities were normalized in the following manner: c-Abl/actin or pY39/[α-syn/actin] or pY125/[α-syn/actin]. The bars represent the mean ± SD of three independent experiments. $^{*}P < 0.01$; $^{**}P < 0.005$ (Student's *t*-test: siRNA Sc cells versus siRNA c-Abl cells). (**C**) c-Abl drug inhibitors protect α-syn from phosphorylation at Y39 and Y125 residues. c-Abl activity can be specifically inhibited using drugs such as nilotinib and imatinib (ATP competitors) or GNF-2 (non-ATP competitor). HEK293T cells were transfected with WT α-syn together with a plasmid encoding for WT c-Abl. Twenty-four hours post-transfection, the cells were left untreated (DMSO) or treated overnight with c-Abl kinase pharmacological inhibitors: nilotinib (20 μM) or imatinib (20 μM) or GNF-2 (20 μM). WB analysis (top panel) shows the decrease of α-syn phosphorylation (Y39 and Y125 residues) when c-Abl activity was inhibited using drugs. Actin was used as a loading control. The phosphorylation of α-syn at residues Y39 and Y125 was evaluated by densitometry quantification (bottom panel). The band intensities were normalized in the following manner: pY39/[α-syn/actin] or pY125/[α-syn/actin]. The bars represent the mean ± SD of three independent experiments. $^{*}P < 0.05$; $^{**}P < 0.005$ (Student's *t*-test: untreated versus c-Abl kinase drug inhibitors). (**D**) c-Abl drug activator DPH induces α-syn phosphorylation at Y39 and Y125 residues in an SH-5Y5 α-syn stable cell line. SH-5Y5 α-syn stable cells were left untreated (DMSO) or treated for 3 h with DPH (50 μM) and analyzed by WB (top panel). DPH induced α-syn phosphorylation at Y39 and Y125 residues was evaluated by densitometry quantification (bottom panel). The band intensities were normalized in the following manner: pY39/[α-syn/actin] or pY125/[α-syn/actin]. The bars represent the mean ± SD of three independent experiments. $^{*}P < 0.05$ (Student's *t*-test: untreated versus DPH treatment). (**E**) c-Abl drug activator induces α-syn phosphorylation at Y39 and Y125 residues. c-Abl activity can be specifically activated using DPH. HEK293T cells were transfected with a siRNA construct against c-Abl or with a control scrambled siRNA (Sc). Twenty-four hours post-transfection, cells were left untreated (DMSO) or treated overnight with c-Abl kinase drugs activator: DPH (50 μM) with or without imatinib (20 μM). Immunoblots (top panel) shown that DPH induced phosphorylation of α-syn (Y39 and Y125 residues) in the cells expressing c-Abl (Sc cells) but not in the cells in which endogenous c-Abl has been downregulated. Imatinib inhibited phosphorylation of α-syn (Y39 and Y125 residues) induced using DPH in the Sc cells. Phosphorylation of α-syn at residues Y39 and Y125 was evaluated by densitometry quantification (bottom panel). The band intensities were normalized in the following manner: pY39/[α-syn /actin] or pY125/[α-syn/actin]. The bars represent the mean ± SD of three independent experiments. $^{**}P < 0.005$ (Student's *t*-test: siRNA Sc cells versus siRNA c-Abl cells).

DPH was also able to induce α-syn phosphorylation at Y39 and Y125 residues in HEK293T transfected with Scramble siRNA (Sc) (Fig. 7E). However, when endogenous c-Abl was downregulated using specific siRNA, the effect of DPH on α-syn phosphorylation was abolished (Fig. 7E). Interestingly, the effect of DPH on α-syn phosphorylation level in HEK293T cells expressing endogenous c-Abl (Sc cells) was inhibited using imatinib (Fig. 7E).

Together, these experiments show that α-syn phosphorylation at Y39 and Y125 can be modulated by regulating c-Abl tyrosine kinase activity using specific inhibitors and activators.

c-Abl interacts with α-syn in primary cortical neurons and in HEK 293T

To determine whether c-Abl directly interacts with α-syn, we performed coimmunoprecipitation experiments of endogenous c-Abl and α-syn using lysates from primary cortical neurons. As shown in Figure 8A, c-Abl was detected in a pull-down of endogenous α-syn. The interaction between α-syn and c-Abl was also confirmed in HEK293T cells co-overexpressing both proteins by immunoprecipitation of either α-syn or c-Abl (Fig. 8B and E). The α-syn that was coimmunoprecipitated with c-Abl was phosphorylated at Y39 and Y125 residues (Fig. 8B and E).

To validate this interaction using a complementary method, we excised the SDS–PAGE band corresponding to c-Abl following immunoprecipitation of α-syn and subjected this sample to tryptic digestion and LC-ESI-MS/MS analysis. Figure 8C shows the sequence coverage for c-Abl, identified from coimmunoprecipitation (right hand panel), and the MS/MS spectrum of a unique c-Abl-specific tryptic peptide (left hand panel). The phosphorylation of α-syn by c-Abl was also confirmed using MS (Fig. 8D). As described above, α-syn was immunoprecipitated from HEK293T cells co-transfected with c-Abl or a control plasmid encoding LUC. The immunoprecipitates were separated using SDS–PAGE, and the bands corresponding to α-syn and c-Abl were excised, digested with trypsin and analyzed by LC–ESI–MS/MS. Figure 8D shows the sequence coverage and a representative MS/MS spectrum confirming α-syn phosphorylation at Y39 residue. Under these conditions, we could not detect any α-syn phosphorylation at the Y125 residue. WB of the immunoprecipitates pulled down using an anti-c-Abl antibody confirmed the interaction with α-syn (Fig. 8E). Moreover, co-immunoprecipitations of α-syn with the c-Abl kinase-dead mutant (KD c-Abl) revealed a lack of interaction between the two proteins, showing that a kinase-active conformation is needed for the interaction (Fig. 8F). Interestingly, mutating Y39, Y125 or both residues to phenylalanine in α-syn did not affect its interaction with c-Abl but only its phosphorylation status (Fig. 8G).

Phosphorylation of α-syn by c-Abl protects against its degradation via the autophagy and proteasome pathways in cortical neurons

To further explore the relationship between α-syn and c-Abl and particularly the mechanisms by which c-Abl expression and/or activation might influence the pathogenicity of α-syn in PD, we investigated the consequences of overexpressing or modulating the activity of c-Abl on α-syn expression levels (mRNA and protein) and its clearance.

Hebron *et al.* have recently suggested a bidirectional relationship between α-syn and c-Abl *in vivo* where an increase of α-syn protein level induces the phosphorylation of c-Abl and thereby its activation, whereas an increase in the c-Abl protein level and activity results in α-syn accumulation (26). In our hands, the overexpression of α-syn in mouse primary cortical neurons using lentiviruses did not induce any changes in c-Abl protein levels (Fig. 9A). We also did not detect an increase in endogenous α-syn expression following the infection of cortical neurons with WT c-Abl lentiviruses (Fig. 9B). As expected, the infection of cortical neurons using WT or PP c-Abl lentiviruses resulted in α-syn phosphorylation at Y39 and Y125 residues (Figs 5 and 9B), whereas KD c-Abl had no effect on α-syn phosphorylation, thus ruling out technical issues during the infection of the neurons (Fig. 9A and B). However, in *in vivo* models in which the α-syn protein level is increased such as in α-syn tg mice (Fig. 3) or in rat midbrain overexpressing α-syn using the AAV-delivery system (Fig. 4), a significant and marked increase in c-Abl protein level (Figs 3B and 4A and B) could be observed. In rat midbrain, the protein levels of c-Abl and activated c-Abl (pY412) are increased (Fig. 4C). Until recently, the endogenous protein levels of c-Abl have been shown to be increased only in the brains of PD patients (26), whereas c-Abl expression in healthy patients remains unchanged (12,13) or at low basal levels (26). Together, these data demonstrate that α-syn overexpression is able to induce the transient expression of c-Abl in the midbrain, consistent with the recently published data of Hebron *et al.* showing an increase of c-Abl protein levels after the overexpression of α-syn in the substantia nigra of mice (26).

Having confirmed that α-syn is phosphorylated at Y39 and Y125 in human brain tissues (Fig. 2A and B), we sought to better understand the physiological consequences of c-Abl-mediated phosphorylation of α-syn. It has previously been reported that phosphorylation of α-syn at S129 regulates its clearance via the proteasome (62) or the autophagy pathways (58). Therefore, we sought to evaluate the neuronal protein levels of α-syn when c-Abl was specifically inhibited. In cortical neurons, α-syn protein levels were dramatically decreased when c-Abl activity was inhibited using nilotinib (Fig. 10A), imatinib or GNF-2 (Supplementary Material, Fig. S5A). c-Abl protein levels were also decreased by nilotinib (Fig. 10A), imatinib or GNF-2 (Supplementary Material, Fig. S5A) treatment. A semi-quantitative RT-PCR assay ruled out any effect of the c-Abl inhibitors on the mRNA levels of α-syn and c-Abl (Fig. 10B, Supplementary Material, Fig. S5B). Interestingly, the effect of nilotinib, the inhibitor showing the highest specificity toward c-Abl inhibition (28), on the α-syn protein levels was counteracted by the proteasome inhibitor MG132 or two inhibitors of autophagy, namely 3-methyladenine (3-MA) 3-MA (a Class III PI 3-kinase inhibitor that inhibits autophagic sequestration at an early stage of autophagy) and bafilomycin A1 (a vacuolar H^+-ATPase inhibitor that blocks late stage autophagy by inhibiting autophagosome fusion to endosomes or lysosomes) (Fig. 10C). However, an inhibitor of lysosomal pathways (NH_4Cl) did not rescue α-syn protein levels after nilotinib treatment (Fig. 10C). The protection of c-Abl from nilotinib-induced degradation was primarily observed upon treatment with bafilomycin A1

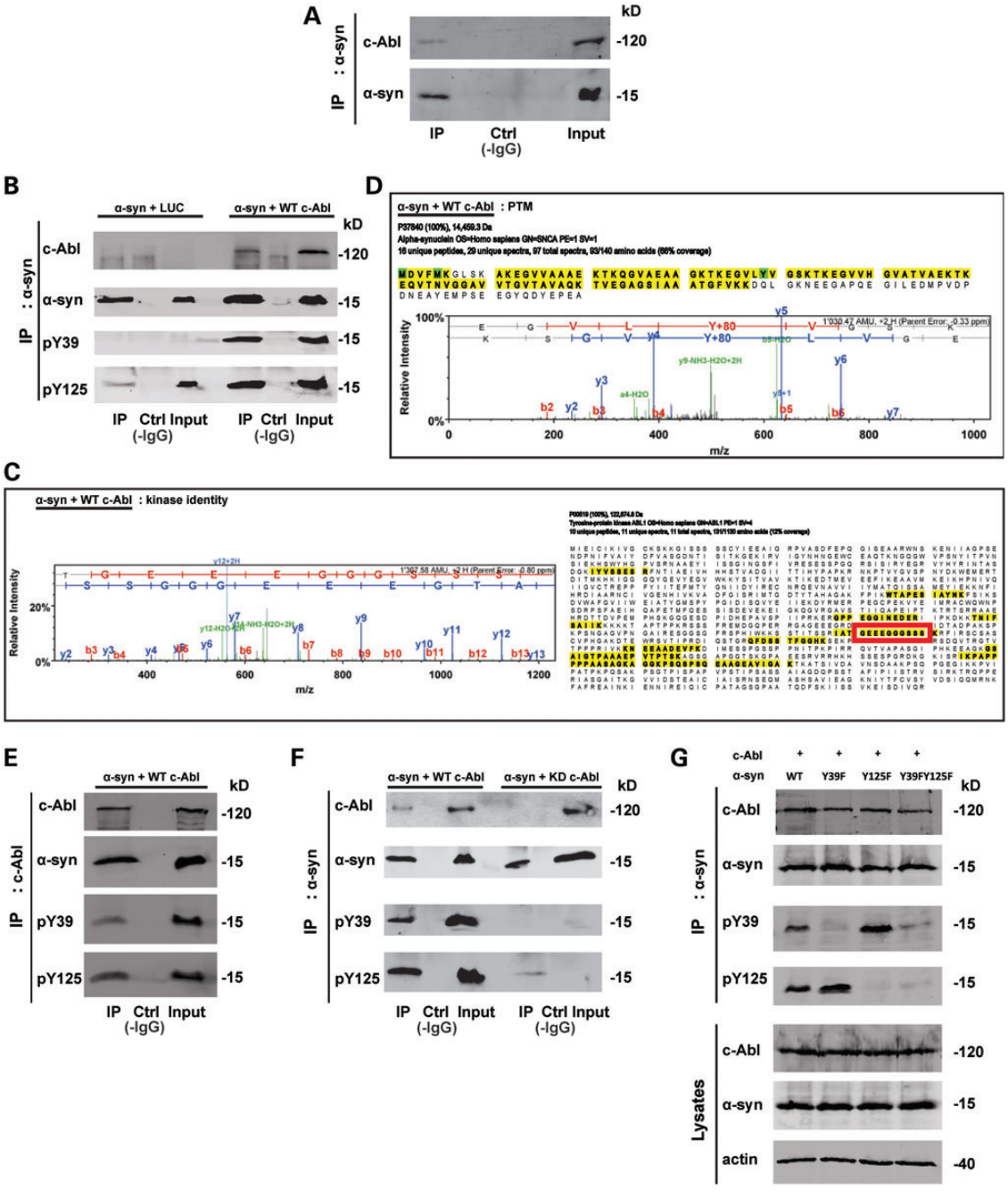

Figure 8. c-Abl interacts with α-syn. (**A**) Co-immunoprecipitation of endogenous/native α-syn and c-Abl. Cortical neurons were lysed and total cell lysates were left untreated (Ctrl without IgG, Input) or immunoprecipitated (IP) with an anti-α-syn antibody and the blots were probed with the indicated antibodies. WB showed that endogenous c-Abl could be co-immunoprecipitated with endogenous α-syn. (**B**–**D**) Mass spectrometry-based confirmation of c-Abl-mediated α-syn phosphorylation at Y39. HEK293T cells were transfected with WT α-syn together with plasmids coding for Luciferase or WT c-Abl. Twenty-four hours post-transfection, total cell lysates were left untreated (Ctrl without IgG, Input) or immunoprecipitated (IP) with an anti-α-syn antibody, and the blots were probed with the indicated antibodies. (B) WB analysis confirmed α-syn phosphorylation at Y39 and Y125 residues and showed c-Abl could be co-immunoprecipitated with α-syn (top panel). IP eluates were also loaded onto Coomassie-stained gels and the bands corresponding to α-syn and c-Abl were excised, digested with trypsin and analyzed by LC–ESI–MS/MS. (C) Sequence coverage for c-Abl identified from the Co-immunoprecipitation, and the MS/MS spectrum of a unique, c-Abl-specific tryptic peptide (sequence GGEEEGGGSSS, indicated by a red frame). (D) The sequence coverage and a representative MS/MS spectrum confirming α-syn phosphorylation at Y39 (figures generated using Scaffold v. 3.4.5). (**E**) α-syn co-immunoprecipitated with c-Abl. HEK293T cells were transfected with WT α-syn together with plasmids encoding for WT c-Abl. Twenty-four hours post-transfection total cell lysates were left untreated (Ctrl without IgG, Input) or immunoprecipitated (IP) with an anti-c-Abl antibody and the blots probed with the indicated antibodies. (**F**) WT c-Abl but not its inactive mutant (KD c-Abl) Co-immunoprecipitated with α-syn. HEK293T cells were transfected with α-syn WT together with plasmids encoding for WT c-Abl or KD c-Abl. Twenty-four hours post-transfection total cell lysates were left untreated (Ctrl without IgG, Input) or IP with an anti-α-syn antibody and blots probed with the indicated antibodies. (**G**) WT c-Abl co-immunoprecipitated with WT α-syn or its mutants. HEK293T cells were transfected with WT α-syn or its mutant (Y39F, Y125F or Y39FY125F) together with plasmid encoding for WT c-Abl. Twenty-four hours post-transfection total cell lysates were left untreated (Ctrl without IgG, Input) or IP with an anti-α-syn antibody, and blots probed with the indicated antibodies.

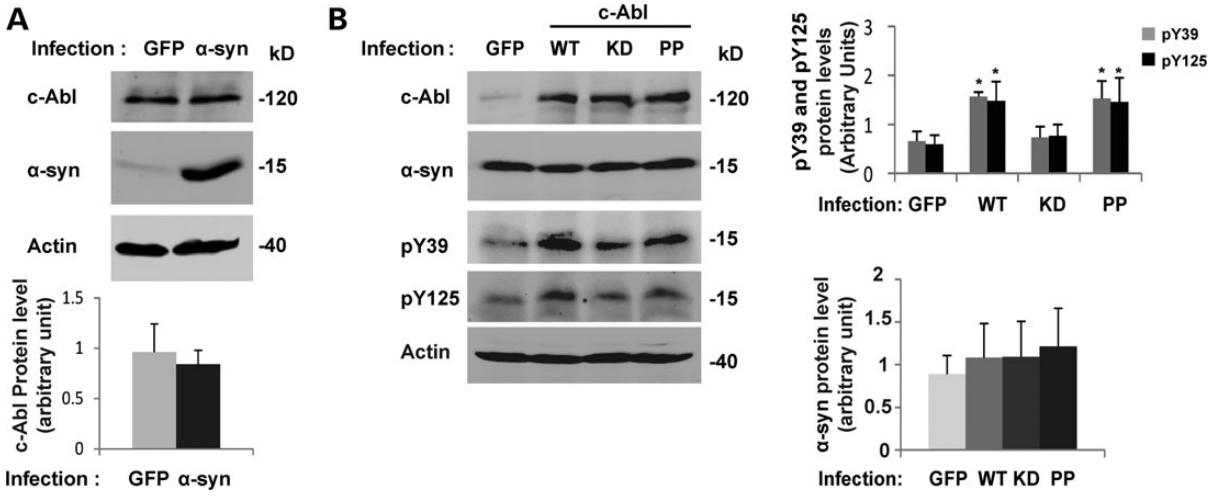

Figure 9. α-syn protein level does not increase in cortical neurons infected by c-Abl. (**A**) Cortical neurons were infected with lentiviruses for GFP or α-syn (top panel). After 5 days, neurons were lysed in Laemmli buffer 2 × and the proteins were separated using SDS–PAGE. The expression levels of α-syn and c-Abl were assessed by WB. Actin was used as a loading control. c-Abl protein level was evaluated by densitometry quantification (bottom panel). The band intensities were normalized in the following manner: (c-Abl/actin). The bars represent the mean ± SD of three independent experiments. $P > 0.05$ (Student's *t*-test: GFP versus α-syn infected cells). (**B**) Cortical neurons were infected with lentiviruses for GFP, WT, KD or PP c-Abl. After 5 days, cells were lysed in Laemmli buffer 2 × and the proteins were separated by SDS–PAGE. α-syn and c-Abl expression levels were assessed by WB (left hand panel). α-syn phosphorylation status was also confirmed using anti-pY39 or pY125 antibodies in a separate protein blot. Actin was used as a loading control. The α-syn protein levels were evaluated by densitometry quantification (right-hand-side panels). The band intensities were normalized in the following manner: (α-syn/actin). The bars represent the mean ± SD of three independent experiments. $P >$ 0.05 (Student's *t*-test:GFP versus c-Abl infected cells); $^{*}P < 0.05$ (Student's *t*-test: GFP versus WT or PP c-Abl infected cells).

(Fig. 10C). Taken together, these results suggest that the inhibition of c-Abl activity leads to the degradation of α-syn *via* autophagy pathways.

DISCUSSION

α-syn is a physiologically relevant substrate for c-Abl

The increased expression or aberrant activation of the tyrosine kinase c-Abl has been implicated in the pathogenesis of PD (12,13,26) and other neurodegenerative diseases (8). In the context of PD, c-Abl-mediated phosphorylation of parkin was shown to inhibit the ubiquitin ligase activity and neuroprotective functions of parkin in primary neuron cultures and in animal models of PD (12,13). The inhibition of c-Abl using imatinib restores the activity and neuroprotective function of parkin. Recently, Hebron *et al.* showed that the pharmacological inhibition of c-Abl promotes the autophagic clearance of α-syn and protects against α-syn-induced loss of dopaminergic neurons in a lentiviral mouse model of synucleinopathies (26,43). However, the role of c-Abl-mediated α-syn phosphorylation in these processes was not known.

Herein, using multiple biophysical and biochemical approaches, we established that c-Abl directly interacts with α-syn and phosphorylates it mostly at Y39 *in vitro* (Fig. 1), and *in vivo* in primary cortical neurons (Fig. 5) and in mammalian cell lines (Figs 6–8). The inhibition of c-Abl activity in cells either by downregulating directly its expression and protein level using siRNA or by inhibiting its kinase activity using specific c-Abl inhibitors such as imatinib, nilotinib or GNF-2 resulted in a strong reduction (∼90%) of Y39 α-syn phosphorylation (Fig. 7C). Conversely, the activation of endogenous c-Abl using DPH induces α-syn phosphorylation at Y39 and Y125 (Fig. 7D and E). These results further demonstrate that α-syn is a *bona fide* substrate for c-Abl.

To explore the relationship between c-Abl and α-syn, and to determine how the interaction between these proteins and Y39 phosphorylation might contribute to the pathogenesis of PD, we assessed and compared the levels of c-Abl, α-syn and Y39 phosphorylation in the brains of PD patients and age-matched controls (Fig. 2). Our results demonstrate for the first time that α-syn phosphorylated at Y39 can be detected in human brain tissues (Fig. 2A and B). However, we did not observe any significant differences in the levels of pY39 and pY125 between PD brains and controls, although c-Abl protein levels were upregulated in PD brains (Fig. 2D). The presence of c-Abl in structures positive for α-syn (Fig. 2C) suggests that the c-Abl interaction and phosphorylation of α-syn might play a role in LB formation and/or the regulation of the pathophysiological properties of α-syn in PD. The investigation of the interplay between α-syn and c-Abl in a rat model of PD also revealed that α-syn overexpression induces a transient induction of c-Abl expression (Fig. 4). All together, these data suggest that c-Abl expression and the accumulation of pY39 could play an important role in modulating α-syn toxicity *in vivo*.

c-Abl and α-syn expression levels are concomitantly regulated: implications for α-syn protein clearance during PD progression

To further explore the interactions between c-Abl and α-syn and gain insights into the mechanisms by which c-Abl expression and/or activation might influence the pathogenicity of α-syn in PD, we investigated the consequences of the overexpression of c-Abl or the enhancement or the inhibition of its kinase activity on the expression and clearance of α-syn. Our results confirmed

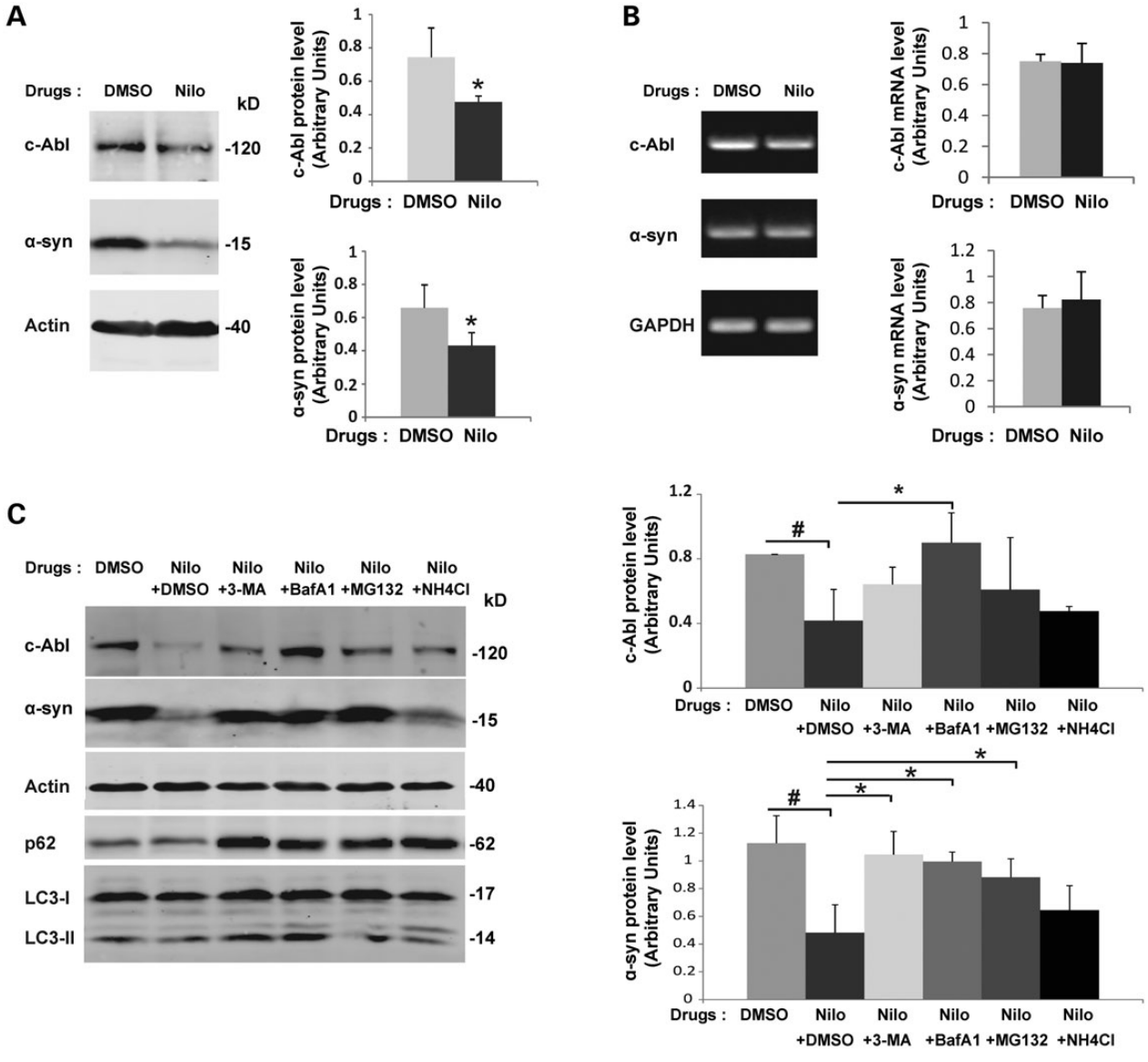

Figure 10. α-syn and c-Abl protein levels are concomitantly regulated via autophagy. (**A**) Inhibition of c-Abl activity by nilotinib induces degradation of α-syn and c-Abl in primary cortical neurons. Primary cultures of cortical neurons were treated with nilotinib or DMSO (negative control). After 16 h of treatment, cells were directly lysed in 2 × Laemmli buffer and the proteins were separated using SDS–PAGE and detected by WB analysis using the appropriate antibodies (left-hand-side panel). Actin was used as a loading control. c-Abl and α-syn protein level were evaluated by densitometry quantification (right-hand-side panels). Band intensities were normalized as in the following manner: (c-Abl/actin) or (α-syn/actin). Bars represent the mean ± SD of three independent experiments. $^{*}P < 0.05$ (Student's *t*-test: DMSO versus nilotinib treatment). (**B**) Inhibition of c-Abl activity by nilotinib does not change mRNA levels of α-syn and c-Abl. Primary cultures of cortical neurons were treated with nilotinib or DMSO (negative control). 16 h post-treatment, cells were lysed and mRNA extraction performed. Semiquantitative RT–PCR using specific primers against c-Abl or α-syn followed by agarose gel electrophoresis (left hand panel) demonstrates that c-Abl and α-syn mRNA levels were not changed upon nilotinib treatment. c-Abl and α-syn mRNA level were evaluated by densitometry quantification (right-hand-side panels). The band intensities were normalized using the mRNA level of the housekeeping gene GAPDH: c-Abl/GAPDH or α-syn/GAPDH. The bars represent the mean ± SD of three independent experiments. $P > 0.05$ (Student's *t*-test: DMSO versus nilotinib). (**C**) Inhibition of c-Abl activity by nilotinib induces degradation of α-syn and c-Abl via the autophagy and proteasome pathways. Primary cultures of cortical neurons were treated with nilotinib or DMSO (negative control) for 16 h prior to addition of inhibitors of autophagy (3-MA, Bafilomycin A1), an inhibitor of phagosome-lysosome fusion (NH_4Cl) or an inhibitor of proteasome (MG-132) for 6 h. The cells were directly lysed in 2 × Laemmli buffer and proteins were separated using SDS–PAGE and detected by WB analysis using the appropriate antibodies (left-hand-side panels). Actin was used as a loading control. c-Abl and α-syn protein levels were evaluated by densitometry quantification (right-hand-side panels). The band intensities were normalized in the following manner: (c-Abl/actin) or (α-syn/actin). The bars represent the mean ± SD of three independent experiments. ANOVA test followed by Tukey–Kramer *post hoc* test were performed: $^{\#}P < 0.05$ (DMSO versus nilotinib) or $^{*}P < 0.05$ (nilotinib ± drugs inhibitors).

previous findings demonstrating that nilotinib induces α-syn protein degradation (Fig. 10A), and that this effect could be reversed when nilotinib is combined with specific inhibitors of autophagy such as 3-MA and Bafilomycin A1, and also using MG132, a proteasome inhibitor (Fig. 10C). Interestingly, not only α-syn protein level decreased in the presence of nilotinib, but c-Abl itself is also targeted for degradation via the autophagy pathway (Fig. 10C). In addition, our results showed that the

overexpression of α-syn in rat midbrain induces a transient upregulation of c-Abl protein level and activity (Fig. 4). These results are in agreement with the recent findings of Hebron *et al.* (26).

Together, our findings suggest that c-Abl-mediated phosphorylation and/or interaction with α-syn plays important roles in stabilizing α-syn by suppressing its clearance via the autophagic and the proteasomal pathways.

Increasing evidence suggests that the tyrosine kinase activity of c-Abl plays important roles in regulating the clearance of key proteins involved in PD or AD and represents a viable target for the treatment of these neurodegenerative disorders. The inhibition of c-Abl activity using different pharmacological inhibitors reduces neurodegeneration in animal models of PD (12,13,26,29). Nilotinib targets not only α-syn but also hyperphosphorylated tau for degradation (26). Imatinib, a first-generation c-Abl inhibitor, has also been shown to act as a powerful activator of autophagy in cells (63), and it inhibits β-amyloid production in rat neuronal primary cultures and in guinea pig brains (64). Further studies are needed to explore the molecular mechanisms underlying the role of c-Abl in regulating the production, clearance and aggregation of these proteins and to validate c-Abl as a target for the treatment of PD and related synucleinopathies.

MATERIALS AND METHODS

Reagents and antibodies

Monoclonal anti-α-syn and monoclonal anti-pY125 were purchased from BD Biosciences (Switzerland). Monoclonal β-actin was from Abcam (Switzerland). Anti-c-Abl (K12), anti-c-Abl (24-11), anti-α/γ/β-syn (N19) and anti-α-syn (211) were obtained from Santa Cruz (Switzerland). Rabbit anti-c-Abl was purchased from Sigma (Switzerland). Custom polyclonal pY39 (raised against the synthetic peptide: K E G V L Y(p) V G S K T K) and polyclonal pY125 were purchased from Eurogentec (Belgium). Monoclonal c-Abl was a gift from Prof. Oliver Hantschel (ISREC Institute, Ecole Polytechnique Fédérale de Lausanne (EPFL), Switzerland). The polyclonal p62 and LC-3 antibodies were a gift from Prof. Darren Moore (EPFL, Switzerland). FL α-syn rabbit polyclonal was from Millipore (Temecula, CA, USA). Secondary antibodies donkey antimouse Alexa^{647}, donkey antirabbit IgG Alexa^{568}, donkey antigoat Alexa^{488} and goat antirabbit Alexa^{680} were purchased from Life Technologies (Switzerland). The secondary antibody goat antimouse IgG IRDye^{800CW} was obtained from Li-Cor Biosciences GmbH (Germany). The secondary antibody antiguinea pig^{HRP} was a gift from Prof. Darren Moore (EPFL, Switzerland). DPH (5-[3-(4-fluorophenyl)-1-phenyl-1H-pyrazol-4-yl]-2,4-imidazolidinedione; c-Abl activator used at a final concentration of 50 μM) 3-MA (3-methyladenine, autophagy inhibitor; used at a final concentration of 10 mM) and NH_4Cl (lysosomal inhibitor; used at a final concentration of 25 mM) were purchased from Sigma-Aldrich (Switzerland). MG-132 (proteasome inhibitor; used at a final concentration of 20 μM) and Bafilomycin A1 (autophagy inhibitor; used at a final concentration of 200 nM) were from Enzo Life Sciences (Switzerland). The c-Abl inhibitors: nilotinib (used at a final concentration of 20 μM), imatinib (used at a final concentration of 20 μM) and GNF-2 (used at a final concentration of 20 μM) were kindly provided by Prof. Oliver Hantschel (ISREC Institute, EPFL, Switzerland).

DNA constructs

Mammalian expression vectors encoding for WT c-Abl, the catalytically inactive mutant of c-Abl (KD c-Abl; K290R) and the constitutively active mutant of c-Abl (PP c-Abl; P242E/P249E) were kindly donated by Prof. Oliver Hantschel (ISREC Institute, EPFL). WT c-Abl, KD c-Abl, PP c-Abl, WT α-syn and GFP were subcloned into the SIN-cPPT-PGK-WHV gateway lentiviral vector kindly provided by Prof. Nicole Déglon (UNIL, Switzerland). Human α-syn was subcloned into the pAAV-CMV vector and the α-syn PD mutants (A30P, E46K, A53T) inserted in the pCDNA6 vector were kindly provided by Prof. Aebischer (Brain Mind Institute, EPFL, Switzerland).

Mass spectrometry

For MS-based analytical phosphorylation assays, 100 μM of WT, Y39F or Y125F α-syn were incubated with 5 μg of recombinant c-Abl in 50 μl of 20 mM Tris, 5 mM $MgCl_2$, 1 mM DTT, 1 mM Na_3VO_4 and 25 mM NaF, pH 7.5, in the presence of 1 mM ATP. Reactions were performed overnight (16 h) at 30°C without agitation. The reaction products were analyzed as intact proteins (i.e. without proteolytic digestion) using LC–ESI–MS on a Thermo LTQ ion trap system and SDS–PAGE/western blotting with primary antibodies indicated where appropriate.

In vitro kinase assays

Recombinant SH2-CD c-Abl kinase was overexpressed and purified from *E.coli* as previously described (65). A total of 100 ng of enzyme was incubated with different biotinylated peptides [CrkL (Y207) peptide: biotin-EPAHAYAQPQTT-amide (calculated Mw: 1538.40 Da, observed Mw: 1537.6 Da), α-syn (Y39): biotin to be replaced by - instead of the underscore KEGV-LYVGSKT, α-syn (Y125): biotin_DPDNEAYEMPS], at various concentrations in the presence of 25 μM ATP for 20 min at room temperature essentially as previously described (66).

For the assays employing FL proteins, recombinant WT and Y39F α-syn were expressed in BL21(DE3) *E. coli* as previously described (67) using a denaturing protocol, with an additional reversed-phase HPLC purification step at the end of the experiment, using a Proto 300 C4 column (20 mm ID × 250 mm length, 5 μm particles) and a gradient from 30 to 60% B over 35 min at 15 ml/min, where solvent A was 0.1% TFA in water and solvent B was 0.1% TFA in acetonitrile. The organic solvents were removed from pooled pure fractions under vacuum using a rotary evaporator and the proteins were subsequently lyophilized and stored at −20°C until use.

For the purification of recombinant CrkII, *E. coli* cells harvested from a 2 l culture expressing his-tagged, FL human CrkII were lysed in in 100 ml Ni-NTA binding buffer (50 mM Tris–HCl, pH 7.5, 500 mM NaCl, 5% glycerol, 25 mM imidazole) using a French press. The lysate was cleared by centrifugation at 14 000*g*, 45 min, 4°C. The cleared lysate was incubated with 1.5 ml Ni-NTA resin (Qiagen) for 2 h and then the slurry

transferred in a gravity flow column (Bio-Rad, Hercules, CA, USA). Beads were washed with 60CV of Ni-NTA binding buffer; then the protein was eluted with the same buffer supplemented with 500 mM Imidazole and several 1.5 ml fractions were collected. After SDS–PAGE analysis, the most concentrated fractions were pooled and further purified. The protein was dialyzed against TEV reaction buffer (50 mM Tris, pH 7.5, 150 mM NaCl, 5% glycerol, 0.5 mM EDTA, 1 mM DTT), then the TEV protease was added at a 1:30 mass ratio and the cleavage reaction proceeded overnight. To purify the TEV cleaved protein, a reverse Ni-NTA purification was performed similarly to previous step. The flowthrough, containing the cleaved protein, was collected and further purified on a HiLoad 26/60 Superdex 75 gel-filtration column (GE Healthcare) in 50 mM Tris–HCl, pH 7.5, 200 mM NaCl, 10% glycerol, 1 mM DTT. The main peak containing the CrkII protein was collected and concentrated using 10 kDa MWCO Microcon spin concentrators (Millipore) for the assay purposes.

Shortly before performing the kinase assays, lyophilized α-syn proteins (WT and Y39F) were resuspended at an initial concentration of about 2 mM in ice-cold, argon-sparged 100 mM Tris, 100 mM NaCl, pH 7.5. Note that the very high protein concentration and TFA counterions resulted in a slight pH drop, requiring manual pH adjustment to 7.5. Because of the tendency of α-syn to self-associate, particularly at high concentration, these stock solutions were kept on ice at all times and rapidly filtered through 100 kDa MWCO Microcon membranes (Millipore) in order to ensure that the kinase assays substrates were in a monomeric state (due to its unfolded nature, α-syn behaves as an ∼50 kDa protein despite its molecular weight of 14.4 kDa, thus only α-syn monomers are able to cross the 100 kDa MWCO membrane). The phosphorylation reactions were carried out at different substrate concentrations, similarly to the assays that used short peptides as substrates as described above. To terminate the reactions, SDS-containing Laemmli sample buffer was added and samples were boiled at 95°C for 5 min, and then resolved on 15% polyacrylamide SDS gels. Gels were then stained overnight at room temperature with a colloidal Coomassie Blue solution, destained against several changes of deionized water for 2 h, then dried under vacuum at 80°C in a Bio-Rad gel dryer. Dried gels were subjected to autoradiography for a first quality control, then α-syn bands were cut, and phosphorylation was quantified by solid-state scintillation counting using a Beckman-Coulter LS6500 multipurpose scintillation counter configured to measure ^{32}P.

Nuclear magnetic resonance

Purified α-syn was obtained from *E. coli* BL21(DE3) cells transfected with plasmids encoding WT α-syn grown in isotopically supplemented minimal media according to previously described protocols (68), purified as previously described (69) and lyophilized. The lyophilized ^{15}N-labeled protein was resuspended in phosphorylation buffer (20 mM Tris, 10 mM $MgCl_2$, 1 mM DTT, pH 6.8) at a concentration of ∼100 μM and then 1 mM ATP and 10 μg SH2-CD c-Abl were added. Sequential 1 h ^{1}H–^{15}N HSQC spectra were collected overnight at 15°C on a Bruker AVANCE 500 MHz spectrometer. The relative intensity of the peaks arising from unphosphorylated and phosphorylated protein was calculated and plotted for well-resolved resonances corresponding to residues in sequential proximity to Y39 (Leu38 and Gly41). All spectra were processed using NMRPipe (70) and analyzed with NMRView (71).

Human brain tissue samples

Samples of the anterior cingulate cortex from longitudinally followed, autopsy-confirmed subjects with PD ($n = 17$; Table 1) and age- and post-mortem delay-matched neurological and neuropathological controls ($n = 17$; Table 1) were obtained from the Sydney Brain Bank and New South Wales Tissue Resource Centre following study approval and with appropriate institutional ethics approval. All PD cases were levodopa-responsive, had no other neurodegenerative conditions and met the UK Brain Bank Clinical Criteria for diagnosis of PD (38). The anterior cingulate cortex was chosen for analysis as this region has been shown to have increased α-syn phosphorylation at the first indication of Lewy body pathologies in the olfactory bulb and substantia nigra (10) with the degree of phosphorylation correlating with the severity of Lewy body formation (11), and has limited cell loss in PD and can therefore be structurally compared with control tissue.

For protein fractionation, human tissue was homogenized in homogenization buffer [0.32 M sucrose, 20 mM Tris–HCl, pH 7.4, 5 mM EDTA, 1× protein inhibitor cocktail (EDTA free; Roche) and 1× phosphatase inhibitor (Roche)], sonicated 2 × 10 s on ice and then cleared by centrifugation at 16 000*g* for 10 min at 4°C. The supernatant was labeled as the TBS-soluble extract (TBS). The pellet was washed twice with homogenization buffer, resuspended in homogenization buffer containing 5% SDS, sonicated for 2 × 10 s and centrifuged at 100 000 *g* for 30 min at 24°C. The supernatant was labeled as the SDS-soluble fraction (SDS). All protein concentrations were determined using the BCA method (Pierce).

For protein detection by WB analysis, 30–60 μg of SDS-soluble protein samples were mixed with 5× Laemmli buffer to obtain a final concentration of 1× per sample in a total volume of 15–40 μl. The samples were denatured at 70°C for 10 min and placed immediately on ice to stop further denaturation of the proteins. The samples were subjected to electrophoresis on 15 and 8% polyacrylamide SDS gels. After separation, the proteins were transferred onto nitrocellulose membranes using the Bio-Rad Trans-Blot Turbo Transfer System. The membranes were blocked with 5% powdered skim milk in TBS-T (10 mM Tris–HCl, pH 7.5, 150 mM NaCl and 0.05% Tween-20) for 1 h. The membranes were then probed overnight using primary antibodies [rabbit polyclonal anti-c-Abl (K-12), rabbit polyclonal anti-pY39-α-syn, rabbit anti-pY125-α-syn, mouse monoclonal anti-α-syn and mouse monoclonal anti-β-actin] diluted in blocking buffer. Finally, the membranes were washed three times in TBS-T buffer and probed with HRP-conjugated secondary antibodies diluted in blocking buffer for 1 h at room temperature (goat antimouse IgG-HRP and goat antirabbit IgG-HRP, Bio-Rad Laboratories). Immunoreactivity was visualized by chemiluminescence using an ECL detection system (GE Healthcare Biosciences) and captured using a Chemidoc imaging system (Bio-Rad).

For protein localization using ICC, 10 μm-thick formalin-fixed paraffin-embedded tissue sections of the anterior cingulate cortex were dewaxed and hydrated, followed by antigen retrieval

in formic acid (90% formic acid for 3 min at room temperature). After washing, the sections were blocked in 50% ethanol containing 5% H_2O_2 for 1 h and then blocked in 5% BSA blocking buffer (0.1% Triton X-100) for 2 h at room temperature. The sections were incubated in primary antibodies [rabbit polyclonal anti-c-Abl (K-12) and mouse monoclonal anti-α-syn (BD)] prepared in 1% BSA blocking buffer (0.02% Triton X-100) overnight at 4°C, followed by detection using an avidin–biotin–peroxidase detection system (Vector Laboratories, Burlingame, CA, USA). The sections were counterstained with 5% cresyl violet to stain Nissl substance and coverslipped with DPX. The images were captured at 40× using an Olympus BH4 microscope with a high-resolution camera. The omission of the primary antibody was used to confirm the specificity of ligand binding.

α-syn tg mice

Mice overexpressing human WT α-syn under the mThy1 promoter (mThy1-α-syn, Line 61) were used (49,54) (6 m/o, $n = 5$ mice per group). This model was selected because the mice develop behavioral motor deficits (40), axonal pathology and accumulation of C-terminus cleaved α-syn and aggregates in cortical and subcortical regions (72) mimicking PD/DLB (55,56). As previously described, brains were homogenized and divided into cytosolic and membrane fractions (56,57). For WB analysis, 20 μg of total protein per lane were loaded into 4–12% Bis–Tris SDS–PAGE gels and blotted onto membranes. Blotted samples from non-tg and α-syn tg mice were probed with the following antibodies: rabbit polyclonal anti-c-Abl (K-12), rabbit polyclonal anti-pY39 α-syn, rabbit anti-pY125 α-syn, FL α-syn rabbit polyclonal (Millipore). Incubation with primary antibodies was followed by species-appropriate incubation with secondary antibodies tagged with horseradish peroxidase (Santa Cruz Biotechnology, Santa Cruz, CA, USA), visualization with enhanced chemiluminescence and analysis with a Versadoc XL imaging apparatus (Bio-Rad). Analysis of β-actin (Sigma-Aldrich, USA) levels was used as a loading control.

ICC analysis was performed in serially sectioned, free-floating, blind-coded vibratome sections. The sections were incubated overnight at 4°C (54) with the following antibodies: rabbit polyclonal anti-c-Abl (K-12), rabbit polyclonal anti-pY39-α-syn, rabbit anti-pY125-α-syn, FL α-syn rabbit polyclonal (Millipore) followed by tagged secondary antibody, avidin biotin HRP and diaminobenzidine reactivity. All sections were processed simultaneously under the same conditions and experiments were performed in triplicate in order to assess the reproducibility of results.

Primary cultures of cortical neurons

Primary cortical neurons were prepared from P0 pups from non-tg mice (C57BL/6JRccHsd, Harlan) or mice lacking α-syn expression (C57BL/6JOlaHsd, Harlan) as previously described (73). Briefly, the cerebral cortices and hippocampi were isolated stereoscopically and dissociated by trituration in medium containing papain (20 U/ml, Sigma-Aldrich). Cortical and hippocampal neurons were cultured in Neurobasal medium containing B27 supplement, L-glutamine and penicillin/streptomycin (Life Technologies). The neurons were seeded on coverslips (CS) previously coated with poly-L-lysine 0.1% (w/v) in water (Sigma-Aldrich) at a density of 150 000 cells/ml (for ICC analysis) or directly plated in 6-well plate for biochemistry analysis at a density of 300 000 cells/ml. After 7 days, the cells were treated with cytosine β-D-arabinofuranoside (Sigma-Aldrich) to a final concentration of 2.3 μM to inhibit glial cell division. The neurons were used after 14 days in culture (2 weeks old).

Lentiviral production and infection of neuronal primary culture

The production and titration of WT, KD, PP c-Abl, WT α-syn and GFP lentiviruses were performed as previously described by Barde *et al.* (74). The final titers for WT α-syn, WT c-Abl and KD c-Abl were 1×10^8 transducing units (TU)/ml and 1×10^9 transducing units (TU)/ml for PP c-Abl and GFP lentiviruses. Cortical primary neurons (2 weeks old) were infected for 5 days with WT c-Abl and KD c-Abl. At Day 5, the neurons were seeded onto CSs and fixed in 4% paraformaldehyde (PFA; Sigma-Aldrich) for 20 min at 4°C and further analyzed by ICC. The neurons plated for biochemistry analysis were treated for 30 min with 100 μM sodium orthovanadate and 4 mM H_2O_2 (Sigma-Aldrich) for 30 min at 37°C to inhibit protein tyrosine phosphatases. The neurons were subsequently lysed in 2× Laemmli buffer and boiled before loading onto a 8% (for c-Abl) or on 15% (for α-syn) SDS–PAGE gels for subsequent detection by WB.

Cell culture and plasmid transfection

HEK293T and HeLa cells were maintained in glutamax-DMEM (Life Technologies) containing 10% FCS (Gibco, Life Technologies), 100 μg/ml of streptomycin and 100 U/ml of penicillin (Life Technologies). Neuroblastoma M17 cells and SH-SY5Y stable cell lines for α-syn were maintained in 50% F-12 and 50% MEM media supplemented in 10% FCS, 100 μg/ml streptomycin and 100 U/ml penicillin (Life Technologies). The SH-S5Y5 stable cell line culture medium was supplemented with 1% G418 (Life Technologies). The 293T cells were transfected using a standard calcium phosphate transfection protocol (75). HeLa and M17 cells were transfected with Effectene (Qiagen, Switzerland) according to the manufacturer's instructions.

c-Abl downregulation with siRNA in HEK293T cells

The following siRNA were purchased from Thermofisher (USA): c-Abl ON-TARGET plus SMARTpool (*L-003100-00*) and ON-TARGETplus Non-targeting Pool (D-001810-10) (scramble). The 293T cells were co-transfected with scramble (Sc) or siRNA against c-Abl with or without plasmids encoding for WT c-Abl and α-syn WT using Jet Prime (Polyplus, France) according to the manufacturer's instructions. At 48 h post-transfection, the cells were lysed and analyzed by WB.

Semiquantitative RT–PCR

Cortical primary neurons were treated for 16 h with nilotinib, imatinib, GNF-2 or DMSO (as a negative control). Cells were then lysed and mRNAs were extracted using RNeasy kit (Qiagen, Switzerland) following the manufacturer's instructions. The

semiquantitative RT–PCR was run using Transcriptor One Step kit (Roche Diagnostic, Switzerland) using the following primers:

GAPDH: FWD 5′-CAGGTTGTCTCCTGCGACTT-3′;
REV 5′-GGCCTCTCTTGCTCAGTGTC-3′
c-Abl: FWD 5′-ACAAAGTGGGCCTCAGCAAG-3′;
REV 5′-CATCTGCTCTGAGTTCCGGG-3
α-syn: FWD 5′-GTGGCTGCTGCTGAGAAAAC-3′;
REV 5′-GAGCAGCCGGCAGATCTTAG-3

The PCR products were loaded onto an agarose gel (1%) stained with SYBR Safe (Life Technologies, Switzerland) and 1 kb plus DNA ladder was used to estimate the size of the band (Fermentas, Switzerland). Images of the agarose gels were acquired with Geni Imager (Syngene, Biolabo, Switzerland).

Immunocytochemistry

HeLa or M17 cells were seeded onto CSs (VWR, Switzerland) and transfected with Effectene (Qiagen) by WT α-syn, Y39F α-syn, Y125F α-syn or Y39F Y125F α-syn together with WT c-Abl or KD c-Abl or PP c-Abl. HEK293T cells were seeded onto CS previously coated with poly-L-lysine (Life Technologies) and transfected using a standard calcium phosphate protocol. Cortical neurons were seeded onto CS previously coated with poly-L-lysine. Mammalian cell lines were grown for 24 h and then fixed in 4% PFA (paraformaldehyde) for 20 min at 4°C. Neurons were fixed in 4% PFA for 10 min at RT. After blocking with 3% BSA (bovine serum albumin) in 0.1% Triton X-100 PBS (phosphate buffer saline) (PBST) for 30 min at room temperature, mammalian cells or cortical primary neurons were incubated with primary antibodies (mouse anti-c-Abl, goat anti-α/γ/β-syn, rabbit anti-pY39-α-syn or rabbit anti-pY125-α-syn) for 1 h at room temperature. The cells were rinsed five times in PBST and subsequently incubated with the secondary antigoat Alexa^{488}, antimouse Alexa^{647} or antirabbit Alexa^{568} at a dilution of 1/800 in PBST. The cells were washed five times in PBST and incubated 30 min at room temperature in DAPI at 2 μg/ml (Life technologies), before mounting in polyvinyl alcohol mounting medium with DABCO (Sigma-Aldrich). The cells were then examined with confocal laser-scanning microscope (LSM 700, Zeiss) with a 20× or a 63× objective and analyzed using Zen software.

Immunohistochemistry of pY39 in tg mice

To investigate the distribution of the phosphorylated α-syn at Y39 *in vivo*, brains from PDGF α-syn tg mice (49), displaying abundant α-syn accumulation in the neocortex and limbic system were analyzed. Control experiments were performed using age-matched α-syn KO mice (76). Consistent with National Institutes of Health (NIH) guidelines for the human treatment of animals, the mice were sacrificed (at 6 months of age) by deep anesthesia with chloral hydrate, and the brains were removed and divided sagittally. Hemibrains were then post-fixed in phosphate-buffered 4% PFA (pH 7.4) at 4°C for 48 h and sectioned at 40 μm using a vibratome 2000 (Leica). The serially sectioned, free-floating, blind-coded vibratome sections were incubated overnight at 4°C with the homemade rabbit polyclonal anti-pY39 α-syn specific antibody (1:250), as previously described (54). The primary antibody incubation was followed by incubation with goat antirabbit IgG (1:100, Vector) followed by avidin D-HRP and DAB revelation. The sections were analyzed with an Olympus bright field microscope.

Cell lysis and WB

Twenty-four hours or 48 h after transfection, the mammalian cell lines and cortical neurons were treated with pervanadate (100 μM sodium orthovanadate and 4 mM H_2O_2) for 20 min at 37°C to inhibit protein tyrosine phosphatases. The mammalian cell lines were then harvested and lysed in 50 mM Tris, pH 7.5; 150 mM NaCl; 1% NP-40; 5 mM EGTA and 5 mM EDTA freshly supplemented with 50 mM NaF, 1 mM sodium orthovanadate; 1 mM PMSF; 10 μg TPCK and 1:200 protease inhibitor mixture (Sigma-Aldrich). The cell lysates were cleared by centrifugation at 4°C for 15 min at 20 000*g*. The total amount of protein in the supernatant was estimated using the BCA^{TM} protein assay kit from Thermo Scientific (Switzerland), according to the manufacturer's instructions. Proteins were diluted in Laemmli buffer 5× (2% SDS, 20% glycerol, 0.05% bromophenol blue, 0.125 M Tris–HCl, pH 6.8, and 5% β-mercaptoethanol). Cortical neurons were directly lysed in 2× Laemmli buffer. The cell lysates were then separated on 8% (c-Abl) or on 15% (pY39, pY125, pS129 and α-syn) SDS–PAGE gels and transferred onto nitrocellulose membrane (Fisher Scientific, Switzerland). The membranes were blocked in Odyssey blocking buffer (Li-Cor Biosciences GmbH, Germany) diluted 1:3 in PBS for 30 min and then incubated with the appropriate antibodies [rabbit polyclonal anti-c-Abl (K-12), rabbit polyclonal anti-pY39-α-syn, mouse anti-pY125-α-syn (BD Transduction Laboratories), mouse monoclonal anti-α-syn and mouse monoclonal anti-β-actin]. The membranes were washed three times in PBS 0.1% Tween and then incubated for 1 h with secondary antibodies (goat anti-(anti-mouse) mouse Alexa^{647}, goat antirabbit Alexa^{647} from Life technologies or goat anti-(anti-mouse) mouse Alexa^{800} from Li-Cor). After three washes with PBS 0.1% Tween, the specific signals were revealed using the Li-Cor scanner at a wavelength of 700 or 800 nm.

Immunoprecipitation, in-gel digestion and MS analyses

Two-week-old cultures of primary cortical neurons grown on 10 cm dishes were lysed in 50 mM Tris, pH 7.5; 150 mM NaCl; 1% NP-40; 5 mM EGTA and 5 mM EDTA freshly supplemented with 50 mM NaF, 1 mM sodium orthovanadate; 1 mM PMSF; 10 μg TPCK and 1:200 protease inhibitor mixture. The cell lysates were cleared by centrifugation at 4°C for 15 min at 20 000*g* followed by two 30 min incubations with protein G-magnetic beads (Millipore, Switzerland). Cleared cell lysates (4 mg) were then incubated overnight at 4°C on a rocking platform without (control) or with 30 μg of anti-α-syn monoclonal (BD Biosciences). The immune complexes were precipitated using 50 μl of protein G-magnetic beads for 1 h at 4°C on a rocking platform and the beads were washed three times with the lysis buffer. The immunoprecipitated proteins were resuspended in 2× Laemmli buffer and boiled before loading onto a 8% (for c-Abl) or 15% (for α-syn) SDS–PAGE gels for subsequent detection by WB.

Forty-eight hours after transfection, HEK293T 293T cells were treated with pervanadate and then lysed as described above. The cell lysates were cleared by centrifugation at 4°C

for 15 min at 20 000*g* followed by two 30 min incubations with protein G-magnetic beads (Millipore, Switzerland). The cell lysates (1 mg) were incubated overnight at 4°C on a rocking platform without (control) or with 10 μg of anti-α-syn monoclonal (BD Biosciences) or 4 μl of anti-c-Abl monoclonal. The immune complexes were precipitated with 50 μl protein G-magnetic beads for 1 h at 4°C on a rocking platform and the beads were washed three times with the lysis buffer. The immunoprecipitated proteins were resuspended in 2× Laemmli buffer and boiled before loading onto 8% (for c-Abl) or 15% (for α-syn) SDS–PAGE gels for subsequent detection by WB or for in gel digestion and MS.

For the in-gel digestion, the bands corresponding to α-syn were excised after Coomassie Blue staining using Simply Blue Safe Stain (Life Technologies). Excised bands were destained with 50% ethanol in 100 mM ammonium bicarbonate (AB), pH 8.4, followed by drying in an evacuated centrifuge, and the proteins were digested in-gel by covering gel pieces with trypsin solution made of 12.5 ng/μl in 50 mM AB (pH 8.4), 10 mM calcium chloride at 37°C overnight. The digested peptides were concentrated to dryness, resuspended in acetonitrile and dried again. After repeating this step once more, the dried peptides were resuspended in 20 μl of 20% formic acid, and 2% acetonitrile, desalted on C_{18} OMIX tips (Agilent Technologies), and analyzed by MALDI–TOF–TOF tandem MS operating in reflector-positive mode on a 4800 series MALDI instrument (AB Sciex) and or on a capillary LC–ESI–MS system (Thermo Scientific LTQ Orbitrap instrument). The collected MS/MS spectra were matched against a human protein database (SwissProt/TrEMBL) and scored using Mascot and Sequest algorithms. The data were then analyzed and presented using Scaffold version 3.0 (Proteome Software).

Plasmid and production of recombinant AAV2/6 viral vectors

The human-syn cDNA and MaxFP-green (FPmax) were cloned into the AAV-CMV-MCS backbone (Stratagene). The production and titration of the recombinant pseudotyped AAV2/6 vectors (serotype 2 genome/serotype 6 capsid) were performed as previously described (72). The final titers were 3.88×10^{10} transducing units (TU)/ml (WT α-syn) and 5.10^{10} TU/ml (FPmax).

Stereotaxic injections

All surgical and behavioral procedures were performed in accordance with the Swiss legislation and the European Community council directive (86/609/EEC) for the care and use of laboratory animals. The injections were performed under xylazine/ketamine anesthesia as described by Paleologou *et al.* (77). Briefly, male Wistar rats (Charles River Laboratories) weighing 180–200 g at the time of surgery were placed in the stereotaxic frame (David Kopf Instruments) and administered a unilateral intranigral injection of 2 μl of viral suspension, which corresponds to a viral load of 1.5×10^7 TU.

Tissue processing and IHC

The animals were deeply anesthetized and transcardially perfused with 4% paraformaldehyde (PFA; Fluka, Sigma-Aldrich) at 13 weeks after injection. The brains were removed, post-fixed for 2 h in 4% PFA, and then placed in 25% sucrose. Coronal sections (25 μm thick) were cut using a microtome (SM2400; Leica) and the slices were stored at −20°C in cryoprotection medium.

ICC analysis was performed as previously described by Paleologou *et al.* (77). The slices were incubated with anti-c-Abl primary antibodies [(K12) and (24-11) from Santa Cruz or from Sigma] and subsequently incubated with biotinylated secondary antibody (1:200; Vector Laboratories) for DAB (3,3-diaminobenzidine) (Pierce) revelation. Imaging was performed on a Leica DMI 4000 microscope (Leica LAS software) equipped with an Olympus AX70 camera.

Relative quantification of WB and statistical analysis

The level of pY39-α-syn or pY125-α-syn was estimated by measuring the WB band intensity using Image J software (National Institute of Health, Bethesda, MD, USA) and normalized to α-syn and the relative pY39-α-syn and pY125-α-syn protein levels were presented as [pY39]/[α-syn/actin] or [pY125]/[α-syn/actin]. The experiments were repeated three times with the same results. The statistical analysis was performed using Student's *t*-test or ANOVA test followed by Tukey–Kramer *post hoc* test. The data were regarded as statistically significant at $P < 0.05$ based on the *t*-test or Tukey–Kramer *post hoc* test.

SUPPLEMENTARY MATERIAL

Supplementary Material is available at *HMG* online.

ACKNOWLEDGEMENTS

We thank Nathalie Jordan for her excellent technical support, Mohamed Bilal Fares and Martial Mbefo Kamdem for their precious help in validating the specificity of our pY39 homemade antibody *in vivo* and by dot blot, respectively, and for their insightful suggestions and discussions. We also thank Prof. Darren Moore for providing the M17 cell line and LC-3 antibody, Nicole Déglon for providing the SIN-cPPT-PGK-WHV gateway lentiviral vector, Diego Chiappe and Romain Hamelin from the Proteomics Core Facility (EPFL, Switzerland) for their precious help for the PTM localization and characterization.

Conflict of Interest statement. None declared.

FUNDING

This work was supported by funding from the EPFL, ERC starting grant (H.A.L., A.L.M.M. and B.F.), Swiss National Science Foundation (H.A.L.) the ISREC Foundation (S.G., A.J.L. and O.H.), National Institute of Health grant R37-AG019391 (D.E and I.D.), Swiss Cancer League (A.J.L. and O.H. KLS-3132-02-2013), National Institute of Health the ISREC Foundation (S.G., A.J.L. and O.H.) and the Swiss Cancer League (A.J.L. and O.H. KLS-3132-02-2013). Brain tissue samples were received from the Sydney Brain Bank at Neuroscience Research Australia and the New South Wales Tissue Resource Centre at the University of Sydney which are supported

by the National Health and Medical Research Council of Australia (NHMRC), University of New South Wales, Neuroscience Research Australia, Schizophrenia Research Institute and National Institute of Alcohol Abuse and Alcoholism (National Institute of Health (NIAAA) R24AA012725). G.M.H. is an NHMRC Senior Principal Research Fellow (#630434).

REFERENCES

1. Moresco, E.M. and Koleske, A.J. (2003) Regulation of neuronal morphogenesis and synaptic function by Abl family kinases. *Curr. Opin. Neurobiol.*, **13**, 535–544.
2. Zukerberg, L.R., Patrick, G.N., Nikolic, M., Humbert, S., Wu, C.L., Lanier, L.M., Gertler, F.B., Vidal, M., Van Etten, R.A. and Tsai, L.H. (2000) Cables links Cdk5 and c-Abl and facilitates Cdk5 tyrosine phosphorylation, kinase upregulation, and neurite outgrowth. *Neuron*, **26**, 633–646.
3. Jones, S.B., Lu, H.Y. and Lu, Q. (2004) Abl tyrosine kinase promotes dendrogenesis by inducing actin cytoskeletal rearrangements in cooperation with Rho family small GTPases in hippocampal neurons. *J. Neurosci.*, **24**, 8510–8521.
4. Woodring, P.J., Litwack, E.D., O'Leary, D.D., Lucero, G.R., Wang, J.Y. and Hunter, T. (2002) Modulation of the F-actin cytoskeleton by c-Abl tyrosine kinase in cell spreading and neurite extension. *J. Cell Biol.*, **156**, 879–892.
5. Lanier, L.M. and Gertler, F.B. (2000) From Abl to actin: Abl tyrosine kinase and associated proteins in growth cone motility. *Curr. Opin. Neurobiol.*, **10**, 80–87.
6. Koleske, A.J., Gifford, A.M., Scott, M.L., Nee, M., Bronson, R.T., Miczek, K.A. and Baltimore, D. (1998) Essential roles for the Abl and Arg tyrosine kinases in neurulation. *Neuron*, **21**, 1259–1272.
7. Moresco, E.M., Scheetz, A.J., Bornmann, W.G., Koleske, A.J. and Fitzsimonds, R.M. (2003) Abl family nonreceptor tyrosine kinases modulate short-term synaptic plasticity. *J. Neurophysiol.*, **89**, 1678–1687.
8. Schlatterer, S.D., Acker, C.M. and Davies, P. (2011) c-Abl in neurodegenerative disease. *J. Mol. Neurosci.*, **45**, 445–452.
9. Cancino, G.I., Toledo, E.M., Leal, N.R., Hernandez, D.E., Yevenes, L.F., Inestrosa, N.C. and Alvarez, A.R. (2008) STI571 prevents apoptosis, tau phosphorylation and behavioural impairments induced by Alzheimer's beta-amyloid deposits. *Brain J. Neurol.*, **131**, 2425–2442.
10. Jing, Z., Caltagarone, J. and Bowser, R. (2009) Altered subcellular distribution of c-Abl in Alzheimer's disease. *J. Alzheimer's Dis.*, **17**, 409–422.
11. Tremblay, M.A., Acker, C.M. and Davies, P. (2010) Tau phosphorylated at tyrosine 394 is found in Alzheimer's disease tangles and can be a product of the Abl-related kinase, Arg. *J. Alzheimer's Dis.*, **19**, 721–733.
12. Ko, H.S., Lee, Y., Shin, J.H., Karuppagounder, S.S., Gadad, B.S., Koleske, A.J., Pletnikova, O., Troncoso, J.C., Dawson, V.L. and Dawson, T.M. (2010) Phosphorylation by the c-Abl protein tyrosine kinase inhibits parkin's ubiquitination and protective function. *Proc. Natl Acad. Sci. USA*, **107**, 16691–16696.
13. Imam, S.Z., Zhou, Q., Yamamoto, A., Valente, A.J., Ali, S.F., Bains, M., Roberts, J.L., Kahle, P.J., Clark, R.A. and Li, S. (2011) Novel regulation of parkin function through c-Abl-mediated tyrosine phosphorylation: implications for Parkinson's disease. *J. Neurosci.*, **31**, 157–163.
14. Alvarez, A.R., Klein, A., Castro, J., Cancino, G.I., Amigo, J., Mosqueira, M., Vargas, L.M., Yevenes, L.F., Bronfman, F.C. and Zanlungo, S. (2008) Imatinib therapy blocks cerebellar apoptosis and improves neurological symptoms in a mouse model of Niemann-Pick type C disease. *FASEB J.*, **22**, 3617–3627.
15. Estrada, L.D., Zanlungo, S.M. and Alvarez, A.R. (2011) C-Abl tyrosine kinase signaling: a new player in AD tau pathology. *Curr. Alzheimer Res.*, **8**, 643–651.
16. Hantschel, O. and Superti-Furga, G. (2004) Regulation of the c-Abl and Bcr-Abl tyrosine kinases. *Nat. Rev. Mol. Cell Biol.*, **5**, 33–44.
17. Sirvent, A., Benistant, C. and Roche, S. (2012) Oncogenic signaling by tyrosine kinases of the SRC family in advanced colorectal cancer. *Am. J. Cancer Res.*, **2**, 357–371.
18. Sun, X., Wu, F., Datta, R., Kharbanda, S. and Kufe, D. (2000) Interaction between protein kinase C delta and the c-Abl tyrosine kinase in the cellular response to oxidative stress. *J. Biol. Chem.*, **275**, 7470–7473.
19. Stuart, J.R., Kawai, H., Tsai, K.K., Chuang, E.Y. and Yuan, Z.M. (2005) c-Abl regulates early growth response protein (EGR1) in response to oxidative stress. *Oncogene*, **24**, 8085–8092.
20. Yuan, Z.M., Shioya, H., Ishiko, T., Sun, X., Gu, J., Huang, Y.Y., Lu, H., Kharbanda, S., Weichselbaum, R. and Kufe, D. (1999) p73 is regulated by tyrosine kinase c-Abl in the apoptotic response to DNA damage. *Nature*, **399**, 814–817.
21. Yoshida, K. (2007) Regulation for nuclear targeting of the Abl tyrosine kinase in response to DNA damage. Adv. Exp. Med. Biol., **604**, 155–165.
22. Zhu, J. and Wang, J.Y. (2004) Death by Abl: a matter of location. *Curr. Top. Dev. Biol.*, **59**, 165–192.
23. Colicelli, J. (2010) ABL tyrosine kinases: evolution of function, regulation, and specificity. *Sci. Signal.*, **3**, re6.
24. Gonfloni, S., Maiani, E., Di Bartolomeo, C., Diederich, M. and Cesareni, G. (2012) Oxidative stress, DNA damage, and c-Abl signaling: at the crossroad in neurodegenerative diseases? *Int. J. Biochem. Cell Biol.*, **2012**, 683097.
25. Alvarez, A.R., Sandoval, P.C., Leal, N.R., Castro, P.U. and Kosik, K.S. (2004) Activation of the neuronal c-Abl tyrosine kinase by amyloid-beta-peptide and reactive oxygen species. *Neurobiol. Dis.*, **17**, 326–336.
26. Hebron, M.L., Lonskaya, I. and Moussa, C.E. (2013) Nilotinib reverses loss of dopamine neurons and improves motor behavior via autophagic degradation of alpha-synuclein in Parkinson's disease models. *Hum. Mol. Genet.*, **22**, 3315–3328.
27. Lin, Y.L., Meng, Y., Jiang, W. and Roux, B. (2013) Explaining why Gleevec is a specific and potent inhibitor of Abl kinase. *Proc. Natl Acad. Sci. USA*, **110**, 1664–1669.
28. Deremer, D.L., Ustun, C. and Natarajan, K. (2008) Nilotinib: a second-generation tyrosine kinase inhibitor for the treatment of chronic myelogenous leukemia. *Clin. Therap.*, **30**, 1956–1975.
29. Imam, S.Z., Trickler, W., Kimura, S., Binienda, Z.K., Paule, M.G., Slikker, W. Jr, Li, S., Clark, R.A. and Ali, S.F. (2013) Neuroprotective efficacy of a new brain-penetrating C-Abl inhibitor in a murine Parkinson's disease model. *PLoS One*, **8**, e65129.
30. Lashuel, H.A., Overk, C.R., Oueslati, A. and Masliah, E. (2013) The many faces of alpha-synuclein: from structure and toxicity to therapeutic target. *Nat. Rev. Neurosci.*, **14**, 38–48.
31. Spillantini, M.G., Crowther, R.A., Jakes, R., Hasegawa, M. and Goedert, M. (1998) alpha-Synuclein in filamentous inclusions of Lewy bodies from Parkinson's disease and dementia with Lewy bodies. *Proc. Natl Acad. Sci. USA*, **95**, 6469–6473.
32. Spillantini, M.G., Schmidt, M.L., Lee, V.M., Trojanowski, J.Q., Jakes, R. and Goedert, M. (1997) Alpha-synuclein in Lewy bodies. *Nature*, **388**, 839–840.
33. Goedert, M. (2001) Alpha-synuclein and neurodegenerative diseases. *Nat. Rev. Neurosci.*, **2**, 492–501.
34. Polymeropoulos, M.H., Lavedan, C., Leroy, E., Ide, S.E., Dehejia, A., Dutra, A., Pike, B., Root, H., Rubenstein, J., Boyer, R. *et al.* (1997) Mutation in the alpha-synuclein gene identified in families with Parkinson's disease. *Science (New York, NY)*, **276**, 2045–2047.
35. Kruger, R., Kuhn, W., Muller, T., Woitalla, D., Graeber, M., Kosel, S., Przuntek, H., Epplen, J.T., Schols, L. and Riess, O. (1998) Ala30Pro mutation in the gene encoding alpha-synuclein in Parkinson's disease. *Nat. Genet.*, **18**, 106–108.
36. Zarranz, J.J., Alegre, J., Gomez-Esteban, J.C., Lezcano, E., Ros, R., Ampuero, I., Vidal, L., Hoenicka, J., Rodriguez, O., Atares, B. *et al.* (2004) The new mutation, E46 K, of alpha-synuclein causes Parkinson and Lewy body dementia. *Ann. Neurol.*, **55**, 164–173.
37. Choi, W., Zibaee, S., Jakes, R., Serpell, L.C., Davletov, B., Crowther, R.A. and Goedert, M. (2004) Mutation E46K increases phospholipid binding and assembly into filaments of human alpha-synuclein. *FEBS Lett.*, **576**, 363–368.
38. Gibb, W.R. and Lees, A.J. (1988) The relevance of the Lewy body to the pathogenesis of idiopathic Parkinson's disease. *J. Neurol. Neurosurg. Psych.*, **51**, 745–752.
39. Appel-Cresswell, S., Vilarino-Guell, C., Encarnacion, M., Sherman, H., Yu, I., Shah, B., Weir, D., Thompson, C., Szu-Tu, C., Trinh, J. *et al.* (2013) Alpha-synuclein p.H50Q, a novel pathogenic mutation for Parkinson's disease. *Mov. Disord.*, **28**, 811–813.
40. Fleming, S.M., Salcedo, J., Fernagut, P.O., Rockenstein, E., Masliah, E., Levine, M.S. and Chesselet, M.F. (2004) Early and progressive sensorimotor anomalies in mice overexpressing wild-type human alpha-synuclein. *J. Neurosci.*, **24**, 9434–9440.

41. Proukakis, C., Dudzik, C.G., Brier, T., MacKay, D.S., Cooper, J.M., Millhauser, G.L., Houlden, H. and Schapira, A.H. (2013) A novel alpha-synuclein missense mutation in Parkinson disease. *Neurology*, **80**, 1062–1064.
42. Lesage, S., Anheim, M., Letournel, F., Bousset, L., Honoré, A., Rozas, N., Pieri, L., Madiona, K., Durr, A., Melki, R. *et al.* (2013) G51D α-synuclein mutation causes a novel Parkinsonian-pyramidal syndrome. *Annals of neurology*, **73**, 459–471.
43. Hebron, M.L., Lonskaya, I. and Moussa, C.E. (2013) Tyrosine kinase inhibition facilitates autophagic SNCA/alpha-synuclein clearance. *Autophagy*, **9**, 1249–1250.
44. Hantschel, O., Grebien, F. and Superti-Furga, G. (2012) The growing arsenal of ATP-competitive and allosteric inhibitors of BCR-ABL. *Cancer Res.*, **72**, 4890–4895.
45. Yang, J., Campobasso, N., Biju, M.P., Fisher, K., Pan, X.Q., Cottom, J., Galbraith, S., Ho, T., Zhang, H., Hong, X. *et al.* (2011) Discovery and characterization of a cell-permeable, small-molecule c-Abl kinase activator that binds to the myristoyl binding site. *Chem. Biol.*, **18**, 177–186.
46. Ellis, C.E., Schwartzberg, P.L., Grider, T.L., Fink, D.W. and Nussbaum, R.L. (2001) alpha-Synuclein is phosphorylated by members of the Src family of protein-tyrosine kinases. *J. Biol. Chem.*, **276**, 3879–3884.
47. Nakamura, T., Yamashita, H., Takahashi, T. and Nakamura, S. (2001) Activated Fyn phosphorylates alpha-synuclein at tyrosine residue 125. *Biochem. Biophys. Res. Commun.*, **280**, 1085–1092.
48. Negro, A., Brunati, A.M., Donella-Deana, A., Massimino, M.L. and Pinna, L.A. (2002) Multiple phosphorylation of alpha-synuclein by protein tyrosine kinase Syk prevents eosin-induced aggregation. *FASEB J.*, **16**, 210–212.
49. Rockenstein, E., Mallory, M., Hashimoto, M., Song, D., Shults, C.W., Lang, I. and Masliah, E. (2002) Differential neuropathological alterations in transgenic mice expressing alpha-synuclein from the platelet-derived growth factor and Thy-1 promoters. *J. Neurosci. Res.*, **68**, 568–578.
50. Feller, S.M., Knudsen, B. and Hanafusa, H. (1994) c-Abl kinase regulates the protein binding activity of c-Crk. *EMBO J.*, **13**, 2341–2351.
51. Bertoncini, C.W., Jung, Y.S., Fernandez, C.O., Hoyer, W., Griesinger, C., Jovin, T.M. and Zweckstetter, M. (2005) Release of long-range tertiary interactions potentiates aggregation of natively unstructured alpha-synuclein. *Proc. Natl Acad. Sci. USA*, **102**, 1430–1435.
52. Lue, L.F., Walker, D.G., Adler, C.H., Shill, H., Tran, H., Akiyama, H., Sue, L.I., Caviness, J., Sabbagh, M.N. and Beach, T.G. (2012) Biochemical increase in phosphorylated alpha-synuclein precedes histopathology of Lewy-type synucleinopathies. *Brain Pathol. (Zurich, Switzerland)*, **22**, 745–756.
53. Walker, D.G., Lue, L.F., Adler, C.H., Shill, H.A., Caviness, J.N., Sabbagh, M.N., Akiyama, H., Serrano, G.E., Sue, L.I. and Beach, T.G. (2013) Changes in properties of serine 129 phosphorylated alpha-synuclein with progression of Lewy-type histopathology in human brains. *Exp. Neurol.*, **240**, 190–204.
54. Masliah, E., Rockenstein, E., Veinbergs, I., Mallory, M., Hashimoto, M., Takeda, A., Sagara, Y., Sisk, A. and Mucke, L. (2000) Dopaminergic loss and inclusion body formation in alpha-synuclein mice: implications for neurodegenerative disorders. *Science (New York, NY)*, **287**, 1265–1269.
55. Games, D., Seubert, P., Rockenstein, E., Patrick, C., Trejo, M., Ubhi, K., Ettle, B., Ghassemiam, M., Barbour, R., Schenk, D. *et al.* (2013) Axonopathy in an alpha-synuclein transgenic model of Lewy body disease is associated with extensive accumulation of C-terminal-truncated alpha-synuclein. *Am. J. Pathol.*, **182**, 940–953.
56. Masliah, E., Rockenstein, E., Veinbergs, I., Sagara, Y., Mallory, M., Hashimoto, M. and Mucke, L. (2001) beta-amyloid peptides enhance alpha-synuclein accumulation and neuronal deficits in a transgenic mouse model linking Alzheimer's disease and Parkinson's disease. *Proc. Natl Acad. Sci. USA*, **98**, 12245–12250.
57. Rockenstein, E., Crews, L. and Masliah, E. (2007) Transgenic animal models of neurodegenerative diseases and their application to treatment development. *Adv. Drug Deliv. Rev.*, **59**, 1093–1102.
58. Oueslati, A., Schneider, B.L., Aebischer, P. and Lashuel, H.A. (2013) Polo-like kinase 2 regulates selective autophagic alpha-synuclein clearance and suppresses its toxicity *in vivo*. *Proceedings of the National Academy of Sciences of the United States of America*, **110**, E3945–3954.
59. Oueslati, A., Paleologou, K.E., Schneider, B.L., Aebischer, P. and Lashuel, H.A. (2012) Mimicking phosphorylation at serine 87 inhibits the aggregation of human alpha-synuclein and protects against its toxicity in a rat model of Parkinson's disease. *J. Neurosci.*, **32**, 1536–1544.
60. Hantschel, O., Rix, U. and Superti-Furga, G. (2008) Target spectrum of the BCR-ABL inhibitors imatinib, nilotinib and dasatinib. *Leuk. Lymphoma*, **49**, 615–619.
61. Adrian, F.J., Ding, Q., Sim, T., Velentza, A., Sloan, C., Liu, Y., Zhang, G., Hur, W., Ding, S., Manley, P. *et al.* (2006) Allosteric inhibitors of Bcr-abl-dependent cell proliferation. *Nat. Chem. Biol.*, **2**, 95–102.
62. Machiya, Y., Hara, S., Arawaka, S., Fukushima, S., Sato, H., Sakamoto, M., Koyama, S. and Kato, T. (2010) Phosphorylated alpha-synuclein at Ser-129 is targeted to the proteasome pathway in a ubiquitin-independent manner. *J. Biol. Chem.*, **285**, 40732–40744.
63. Ertmer, A., Huber, V., Gilch, S., Yoshimori, T., Erfle, V., Duyster, J., Elsasser, H.P. and Schatzl, H.M. (2007) The anticancer drug imatinib induces cellular autophagy. *Leukemia*, **21**, 936–942.
64. Netzer, W.J., Dou, F., Cai, D., Veach, D., Jean, S., Li, Y., Bornmann, W.G., Clarkson, B., Xu, H. and Greengard, P. (2003) Gleevec inhibits beta-amyloid production but not Notch cleavage. *Proc. Natl Acad. Sci. USA*, **100**, 12444–12449.
65. Seeliger, M.A., Young, M., Henderson, M.N., Pellicena, P., King, D.S., Falick, A.M. and Kuriyan, J. (2005) High yield bacterial expression of active c-Abl and c-Src tyrosine kinases. *Protein Sci.*, **14**, 3135–3139.
66. Hantschel, O., Warsch, W., Eckelhart, E., Kaupe, I., Grebien, F., Wagner, K.U., Superti-Furga, G. and Sexl, V. (2012) BCR-ABL uncouples canonical JAK2-STAT5 signaling in chronic myeloid leukemia. *Nat. Chem. Biol.*, **8**, 285–293.
67. Fauvet, B., Mbefo, M.K., Fares, M.B., Desobry, C., Michael, S., Ardah, M.T., Tsika, E., Coune, P., Prudent, M., Lion, N. *et al.* (2012) alpha-Synuclein in central nervous system and from erythrocytes, mammalian cells, and Escherichia coli exists predominantly as disordered monomer. *J. Biol. Chem.*, **287**, 15345–15364.
68. Eliezer, D., Kutluay, E., Bussell, R. Jr. and Browne, G. (2001) Conformational properties of alpha-synuclein in its free and lipid-associated states. *J. Mol. Biol.*, **307**, 1061–1073.
69. Fauvet, B., Fares, M.B., Samuel, F., Dikiy, I., Tandon, A., Eliezer, D. and Lashuel, H.A. (2012) Characterization of semisynthetic and naturally Nalpha-acetylated alpha-synuclein in vitro and in intact cells: implications for aggregation and cellular properties of alpha-synuclein. *J. Biol. Chem.*, **287**, 28243–28262.
70. Delaglio, F., Grzesiek, S., Vuister, G.W., Zhu, G., Pfeifer, J. and Bax, A. (1995) NMRPipe: a multidimensional spectral processing system based on UNIX pipes. *J. Biomol. NMR*, **6**, 277–293.
71. Johnson, B.A., Stevens, S.P. and Williamson, J.M. (1994) Determination of the three-dimensional structure of margatoxin by 1H, 13C, 15N triple-resonance nuclear magnetic resonance spectroscopy. *Biochemistry*, **33**, 15061–15070.
72. Azeredo da Silveira, S., Schneider, B.L., Cifuentes-Diaz, C., Sage, D., Abbas-Terki, T., Iwatsubo, T., Unser, M. and Aebischer, P. (2009) Phosphorylation does not prompt, nor prevent, the formation of alpha-synuclein toxic species in a rat model of Parkinson's disease. *Hum. Mol. Gen.*, **18**, 872–887.
73. Steiner, P., Sarria, J.C., Glauser, L., Magnin, S., Catsicas, S. and Hirling, H. (2002) Modulation of receptor cycling by neuron-enriched endosomal protein of 21 kD. *J. Cell Biol.*, **157**, 1197–1209.
74. Barde, I., Salmon, P. and Trono, D. (2010) Production and titration of lentiviral vectors. *Curr. Prot. Neurosci.* Chapter 4, Unit 4, p. 21.
75. Wigler, M., Silverstein, S., Lee, L.S., Pellicer, A., Cheng, Y. and Axel, R. (1977) Transfer of purified herpes virus thymidine kinase gene to cultured mouse cells. *Cell*, **11**, 223–232.
76. Abeliovich, A., Schmitz, Y., Farinas, I., Choi-Lundberg, D., Ho, W.H., Castillo, P.E., Shinsky, N., Verdugo, J.M., Armanini, M., Ryan, A. *et al.* (2000) Mice lacking alpha-synuclein display functional deficits in the nigrostriatal dopamine system. *Neuron*, **25**, 239–252.
77. Paleologou, K.E., Oueslati, A., Shakked, G., Rospigliosi, C.C., Kim, H.Y., Lamberto, G.R., Fernandez, C.O., Schmid, A., Chegini, F., Gai, W.P. *et al.* (2010) Phosphorylation at S87 is enhanced in synucleinopathies, inhibits alpha-synuclein oligomerization, and influences synuclein-membrane interactions. *J. Neurosci.*, **30**, 3184–3198.